Bending, vibration, buckling analysis of bi-directional FG porous microbeams with a variable material length scale parameter

Armagan Karamanli[a], Thuc P. Vo[b,*]

[a]Faculty of Engineering and Natural Sciences, Mechatronics Engineering, Bahcesehir University, Istanbul, Turkey.

[b]School of Engineering and Mathematical Sciences, La Trobe University, Bundoora, VIC 3086, Australia

[*]Corresponding author. E-mail: t.vo@latrobe.edu.au (T P Vo)

Abstract

Finite elemen model for the structural behaviours of bi-directional (2D) FG porous microbeams based on a quasi-3D theory and the modified strain gradient theory (MSGT) is presented. As the main novelty of this study, in order to capture accurately the size effects, the MSGT is employed with three material length scale parameters (MLSPs) rather than the modifed couple stress theory (MCST) with only one MLSP. The material properties including three MLSPs are varied in both the axial and thickness directions as well as porosity. By using a quasi-3D theory, which inludes normal and shear deformations, the governing equations for static, vibration and buckling analysis are derived and solved by Hermite-cubic beam element for various boundary conditions. Through numerical examples, effects of variable MLSP and porosity as well as gradient index in two directions on the deflections, natural frequencies and buckling loads of 2D FG porous microbeams are examined.

Keywords: 2D FG porous microbeams; Modified strain gradient theory; Bending; Buckling; Vibration

1. Introduction

Nowadays, Functionally Graded Materials (FGMs) can be used in the micro/nanoelectromechanical systems [1, 2], shape memory alloy thin films [3-5] and atomic force microscopes [6], etc. At micro and nano-scale level, it is well-known that their responses are size-dependent [7-9] thus classical continuum elasticity fail to capture. By introducing the Material Length Scale Parameters (MLSP) in the constitutive relations, many theories on have been proposed for example the Modified Couple Stress Theory (MCST) [10], Modified Strain Gradient Theory (MSGT) [11], micropolar theory [12], nonlocal elasticity theory [13], and so on. Based on the MSGT, many size-dependent models were developed for the FG microbeams using various theories such as Classical Beam Theory (CBT) [14-18], First-Order Beam Theory (FBT) [19-23] and higher-order beam theory including Third-order Beam Theory (TBT) [24-27], Sinusoidal Beam Theory (SBT) [28-31]. Some of them are mentioned here since a comprehensive review related to this topic was carried out by Thai et al. [32] and Ghayesh & Farajpour [33]. It should be mentioned that the MLSP is considered as constant as ℓ = 15μm in all works on the FG microbeams mentioned above. Literature review shows that it has different values depending on materials [34-37], for example homogeneous epoxy ℓ = 17,6μm [11], cold-worked polycrystalline copper ℓ = 5,84μm [38]. Thus, the MLSP should be variable when dealing with the FG microbeams. There are few papers that consider the variation of MLSP through the thickness similar to other material properties. The only work using the MSGT seems to be that by Kahrobaiyan et al. [39] who studied their size-dependent bending and vibration analysis using the CBT. By using the MCST, Aghazadeh et al. [40] used of the differential quadrature method (DQM) to solve static and vibration responses of the FG microbeams with various beam theories. AlBasyouni et al. [41] employed neutral surface position to develop Navier solutions for deflection and frequency of the FG microbeams. Babaei et al. [42] and Babaei & Rahmani [43] studied temperature-dependent vibration analysis of the FG microbeams using the CBT and FBT. It should be noted here that all above references focused on the responses of conventional FGMs, whose material properties vary only through the thickness. NematAlla [44] showed that bi-directional (2D) FGMs were effective in design industrial machine elements such as modern aerospace shuttles, craft than conventional one since they can reduce thermal and residual stresses. Besides, in their fabrication process, micro voids or porosities can happen during a multi-step sequential infiltration technique [45] or during the process of sintering [46]. Therefore, it is important to investigate size-dependent responses of 2D FG porous microbeams using variable MLSP.

Although there are large amount studies on the FG microbeams, only a few research related to 2D FG microbeams and all of them used the MCST. Shafiei et al. [47, 48] used the DQM to investigate vibration of 2D FG porous Timoshenko nano/microbeams and buckling response of 2D FG tapered Euler-Bernoulli nano/microbeams. By using a quasi-3D (Q3D) theory, Trinh et al. [49] used the state-space concept to solve the natural frequencies of 2D FG microbeams. Yu et al. [50] developed isogeometric analysis for vibration and bending analysis of 2D FG microbeams. Karamanli and his colleagues applied finite element model (FEM) to investigate bending analysis [51], flapwise vibration analysis [52] and buckling analysis [53] of 2D FG porous microbeams using the MCST. In order to consider variable MLSP, Chen et al. [54, 55] considered three models of variable MLSP to investigate vibration, buckling and postbuckling responses of 2D FG microbeams using a TBT. From above reports, the studies related to 2D FG porous microbeams are still very limited in the literature. Their results based on the MSGT and Q3D theory are not available. For those reasons, a combination of the MSGT, Q3D and FEM is an interesting topic and has not been studied yet. Thus, the main objective is to develop a size dependent FEM for analysis of 2D FG porous microbeams.

In this work, the MSGT with three variable MLSPs is employed to capture the size effects of 2D FG porous microbeams using a Q3D theory. All material properties including the MLSPs are varied through both axial and thickness as well as porosity coefficient. The governing equations for static, vibration and buckling analysis are derived by using the Lagrange's equations and solved by Hermite-cubic beam element. The verification is performed by comparing the numerical results with those from the MCST. Two porosity models including even and uneven are considered to investigate the effects of variable MLSP, porosity coefficient, gradient index in two directions, and boundary conditions on the structural responses of 2D FG porous microbeams.

2. 2D FG Porous Microbeams

The geometry and dimensions of 2D FG microbeams with two porosity models namely FGM I and FGM II [56] is illustrated in Fig. 1. Their Young's modulus $E(x,z)$, Poisson's ratio $\nu(x,z)$, mass density $\rho(x,z)$ and MLSP $\ell(x,z)$ can be expressed by using the rule of mixture as:

$$P(x,z) = P_c\left(V_c(x,z) - \frac{\alpha_0(z)}{2}\right) + P_m\left(V_m(x,z) - \frac{\alpha_0(z)}{2}\right) \qquad (1a)$$

$$V_c(z) = \left(\frac{1}{2} + \frac{z}{h}\right)^{p_z}\left(\frac{x}{L}\right)^{p_x} \text{ and } V_c(x,z) + V_m(x,z) = 1 \qquad (1b)$$

where P_c, P_m and V_c, V_m are material property and volume fraction of ceramic and metal. Besides, p_x and p_z are material gradient index in the axial and thickness direction and α_0 is porosity coefficient.

The effective material properties for each model can be presented by [57]:

FGM I (Even)

$$E(x,z) = (E_c - E_m)\left(\frac{1}{2} + \frac{z}{h}\right)^{p_z}\left(\frac{x}{L}\right)^{p_x} + E_m - \frac{\alpha_0}{2}(E_c + E_m) \qquad (2a)$$

$$\nu(x,z) = (\nu_c - \nu_m)\left(\frac{1}{2} + \frac{z}{h}\right)^{p_z}\left(\frac{x}{L}\right)^{p_x} + \nu_m - \frac{\alpha_0}{2}(\nu_c + \nu_m) \qquad (2b)$$

$$\rho(x,z) = (\rho_c - \rho_m)\left(\frac{1}{2} + \frac{z}{h}\right)^{p_z}\left(\frac{x}{L}\right)^{p_x} + \rho_m - \frac{\alpha_0}{2}(\rho_c + \rho_m) \qquad (2c)$$

$$\ell(x,z) = (\ell_c - \ell_m)\left(\frac{1}{2} + \frac{z}{h}\right)^{p_z}\left(\frac{x}{L}\right)^{p_x} + \ell_m - \frac{\alpha_0}{2}(\ell_c + \ell_m) \qquad (2d)$$

FGM II (Uneven)

$$E(x,z) = (E_c - E_m)\left(\frac{1}{2}+\frac{z}{h}\right)^{p_z}\left(\frac{x}{L}\right)^{p_x} + E_m - \frac{\alpha_0}{2}\left(1-\frac{2|z|}{h}\right)(E_c + E_m) \tag{3a}$$

$$\nu(x,z) = (\nu_c - \nu_m)\left(\frac{1}{2}+\frac{z}{h}\right)^{p_z}\left(\frac{x}{L}\right)^{p_x} + \nu_m - \frac{\alpha_0}{2}\left(1-\frac{2|z|}{h}\right)(\nu_c + \nu_m) \tag{3b}$$

$$\rho(x,z) = (\rho_c - \rho_m)\left(\frac{1}{2}+\frac{z}{h}\right)^{p_z}\left(\frac{x}{L}\right)^{p_x} + \rho_m - \frac{\alpha_0}{2}\left(1-\frac{2|z|}{h}\right)(\rho_c + \rho_m) \tag{3c}$$

$$\ell(x,z) = (\ell_c - \ell_m)\left(\frac{1}{2}+\frac{z}{h}\right)^{p_z}\left(\frac{x}{L}\right)^{p_x} + \ell_m - \frac{\alpha_0}{2}\left(1-\frac{2|z|}{h}\right)(\ell_c + \ell_m) \tag{3d}$$

Variations of Young's modulus of FGM I and MLSP of FGM II in *x* and *z*-directions with p_x=p_z=1, 2 and 10 are plotted in Fig. 2.

3. Variational Formulation

By using the MSGT [11], the strain energy ($\mathcal{U}$) can be expressed:

$$\mathcal{U} = \frac{1}{2}\int_V (\sigma_{ij}\varepsilon_{ij} + m_{ij}\chi_{ij} + p_i\gamma_i + \tau_{ijk}\eta_{ijk})d\,\mathcal{V}, \quad i,j,k = 1,2,3 \tag{4}$$

where σ_{ij} is the stress tensor, ε_{ij} is the strain tensor, m_{ij} is the deviatoric part of the symmetric couple stress tensor and χ_{ij} is the symmetric curvature tensor, γ_i is the dilatation gradient tensor, η_{ijk} is the deviatoric stretch gradient tensor and p_i and τ_{ijk} are the higher order stress tensors associated with the dilatation gradient and deviatoric stretch gradient tensors.

Based on the displacement field (u_1, u_2, u_3), the strain tensors can be presented as follows:

$$\varepsilon_{ij} = \frac{1}{2}\left(\frac{\partial u_i}{\partial x_j} + \frac{\partial u_j}{\partial x_i}\right) \tag{5a}$$

$$\chi_{ij} = \frac{1}{4}\left(e_{imn}\frac{\partial^2 u_n}{\partial x_{mj}^2} + e_{jmn}\frac{\partial^2 u_n}{\partial x_{mi}^2}\right) \tag{5b}$$

$$\gamma_i = \frac{\partial \varepsilon_{mm}}{\partial x_i} \tag{5c}$$

$$\eta_{ijk} = \frac{1}{3}\left(\frac{\partial \varepsilon_{jk}}{\partial x_i} + \frac{\partial \varepsilon_{ki}}{\partial x_j} + \frac{\partial \varepsilon_{ij}}{\partial x_k}\right) - \frac{1}{15}\left[\delta_{ij}\left(\frac{\partial \varepsilon_{mm}}{\partial x_k} + 2\frac{\partial \varepsilon_{mk}}{\partial x_m}\right) + \delta_{jk}\left(\frac{\partial \varepsilon_{mm}}{\partial x_i} + 2\frac{\partial \varepsilon_{mi}}{\partial x_m}\right) + \delta_{ki}\left(\frac{\partial \varepsilon_{mm}}{\partial x_j} + 2\frac{\partial \varepsilon_{mj}}{\partial x_m}\right)\right] \quad (5d)$$

where e_{ijk} and δ_{ij} denote the permutation symbol and Kronecker delta.

Constitutive relations between stress and strain tensors:

$$\sigma_{ij} = \left(\frac{E(x,z)}{1+\nu(x,z)}\right)\varepsilon_{ij} + \left[\frac{\nu(x,z)E(x,z)}{(1+\nu(x,z))(1-2\nu(x,z))}\right]\varepsilon_{kk}\delta_{ij} \quad (6a)$$

$$p_i = \left(\frac{E(x,z){\ell_0}^2(x,z)}{1+\nu(x,z)}\right)\gamma_i \quad (6b)$$

$$\tau_{ijk} = \left(\frac{E(x,z){\ell_1}^2(x,z)}{1+\nu(x,z)}\right)\eta_{ijk} \quad (6c)$$

$$m_{ij} = \left(\frac{E(x,z){\ell_2}^2(x,z)}{1+\nu(x,z)}\right)\chi_{ij} \quad (6d)$$

where ℓ_0, ℓ_1 and ℓ_2 are three MLSPs related to the dilatation gradient, deviatoric stretch gradient and symmetric curvature.

By using a Q3D theory, the displacement fields can be expressed [47-49] as:

$$u_1(x,z,t) = U(x,z,t) = u(x,t) - f_1(z)\frac{\partial w_b(x,t)}{\partial x} + f_2(z)\frac{\partial w_s(x,t)}{\partial x} \quad (7a)$$

$$u_3(x,t) = W(x,t) = w_b(x,t) + w_s(x,t) + f_3(z)\, w_z(x,t) \quad (7b)$$

$$f_1(z) = \frac{4z^3}{3h^2}, f_2(z) = z - \frac{8z^3}{3h^2} \ \ and \ \ f_3(z) = 1 - \frac{4z^2}{h^2} \quad (7c)$$

where $u, w_b, w_s \ and \ w_z$ are the axial displacement and bending, shear and thickness stretching components of the vertical displacement.

The only nonzero strains can be obtained:

$$\varepsilon_x = \frac{\partial U}{\partial x} = u' - f_1 w_b'' + f_2 w_s'' \quad (8a)$$

$$\varepsilon_z = \frac{\partial W}{\partial z} = {f_3}' w_z \quad (8b)$$

$$\varepsilon_{xz} = \frac{\gamma_{xz}}{2} = \frac{\partial W}{\partial x} + \frac{\partial U}{\partial z} = \frac{1}{2} f_3(w_b' + 2w_s' + w_z') \tag{8c}$$

The components of the strain tensor associated with the higher order stresses can be given by using Eq. (5):

$$\chi_{xy} = \frac{1}{4}[-(1+f_1{}')w_b'' - (1-f_2{}')w_s'' - f_3 w_z''] \tag{9a}$$

$$\chi_{yz} = \frac{1}{2}\left(\frac{\partial \theta_z}{\partial y} + \frac{\partial \theta_y}{\partial z}\right) = \frac{1}{4}(-f_1{}''w_b' + f_2{}''w_s' - f_3{}'w_z') \tag{9b}$$

$$\gamma_x = u'' - f_1 w_b''' + f_2 w_s''' + f_3{}'w_z' \tag{9c}$$

$$\gamma_z = -f_1{}'w_b'' + f_2{}'w_s'' + f_3{}''w_z \tag{9d}$$

$$\eta_{xxx} = \frac{1}{5}[2u'' - 2f_1 w_b''' - f_3{}'w_b' + 2f_2 w_s''' - 2f_3{}'w_s' - f_3{}'w_z'] \tag{9e}$$

$$\eta_{zzz} = \frac{1}{5}[f_1{}'w_b'' - f_3 w_b'' - f_2{}'w_s'' - 2f_3 w_s'' + 2f_3{}''w_z - f_3 w_z''] \tag{9f}$$

$$\eta_{yyx} = \eta_{yxy} = \eta_{xyy} = \frac{1}{15}[-3u'' + 3f_1 w_b''' - f_3{}'w_b' - 3f_2 w_s''' - 2f_3{}'w_s' - 2f_3{}'w_z'] \tag{9g}$$

$$\eta_{zzx} = \eta_{zxz} = \eta_{xzz} = \frac{1}{15}[-3u'' + 3f_1 w_b''' + 4f_3{}'w_b' - 3f_2 w_s''' + 8f_3{}'w_s' + 8f_3{}'w_z'] \tag{9h}$$

$$\eta_{xxz} = \eta_{xzx} = \eta_{zxx} = \frac{1}{15}[-4f_1{}'w_b'' + 4f_3 w_b'' + 8f_3 w_s'' + 4f_2{}'w_s'' + 4f_3 w_z'' - 3f_3{}''w_z] \tag{9i}$$

$$\eta_{yyz} = \eta_{yzy} = \eta_{zyy} = \frac{1}{15}[f_1{}'w_b'' - f_3 w_b'' - f_2{}'w_s'' - 2f_3 w_s'' - 3f_3{}''w_z - f_3 w_z''] \tag{9j}$$

$$\chi_{xx} = \chi_{yy} = \chi_{zz} = \chi_{xz} = \gamma_y = \eta_{zzy} = \eta_{zyz} = \eta_{yzz} = \eta_{yyy} = \eta_{xyz} = \eta_{yzx} = \eta_{zxy} = \eta_{xzy} = \eta_{zyx} = \eta_{yxz} = 0 \quad (9k)$$

Constitutive relations between stress and strains of 2D FG microbeams:

$$\begin{Bmatrix} \sigma_x \\ \sigma_z \\ \sigma_{xz} \end{Bmatrix} = \begin{bmatrix} Q_{11} & Q_{13} & 0 \\ Q_{13} & Q_{33} & 0 \\ 0 & 0 & Q_{44} \end{bmatrix} \begin{Bmatrix} \varepsilon_x \\ \varepsilon_z \\ 2\varepsilon_{xz} \end{Bmatrix} \quad (10a)$$

$$Q_{11}(x,z) = Q_{33}(x,z) = \frac{E(x,z)}{(1 - v^2(x,z))} \quad (10b)$$

$$Q_{13}(x,z) = \frac{E(x,z)v(x,z)}{(1 - v^2(x,z))} \quad (10c)$$

$$Q_{44}(x,z) = \frac{E(x,z)}{2(1 + v(x,z))} \quad (10d)$$

$$\begin{Bmatrix} p_x \\ p_z \end{Bmatrix} = \frac{E(x,z){\ell_0}^2(x,z)}{1 + \nu(x,z)} \begin{Bmatrix} \gamma_x \\ \gamma_z \end{Bmatrix} \quad (10e)$$

$$\begin{Bmatrix} \tau_{xxx} \\ \tau_{zzz} \\ \tau_{xyy} \\ \tau_{xzz} \\ \tau_{zxx} \\ \tau_{zyy} \end{Bmatrix} = \frac{E(x,z){\ell_1}^2(x,z)}{1 + \nu(x,z)} \begin{Bmatrix} \eta_{xxx} \\ \eta_{zzz} \\ \eta_{xyy} \\ \eta_{xzz} \\ \eta_{zxx} \\ \eta_{zyy} \end{Bmatrix} \quad (10f)$$

$$\begin{Bmatrix} m_{xy} \\ m_{yz} \end{Bmatrix} = \frac{E(x,z){\ell_2}^2(x,z)}{1 + \nu(x,z)} \begin{Bmatrix} \chi_{xy} \\ \chi_{yz} \end{Bmatrix} \quad (10g)$$

Based on the displacement field given in Eq. (7), the following expression of $\mathcal{U}$ can be derived by substituting Eq. (10):

$$\mathcal{U} = \frac{1}{2}\int_V (\sigma_x\varepsilon_x + \sigma_z\varepsilon_z + \sigma_{xz}\gamma_{xz} + p_x\gamma_x + p_z\gamma_z + \tau_{xxx}\eta_{xxx} + \tau_{zzz}\eta_{zzz} + 3\tau_{xyy}\eta_{xyy} + 3\tau_{xzz}\eta_{xzz} + 3\tau_{zxx}\eta_{zxx} + 3\tau_{zyy}\eta_{zyy} + 2m_{xy}\chi_{xy} + 2m_{yz}\chi_{yz})dV \quad (11a)$$

$$\mathcal{U} = \frac{1}{2}\int_V \left[(Q_{11}{\varepsilon_x}^2 + 2Q_{13}\varepsilon_x\varepsilon_z + Q_{11}{\varepsilon_z}^2 + Q_{44}{\gamma_{xz}}^2) + \frac{E{\ell_0}^2}{1+\nu}({\gamma_x}^2 + {\gamma_z}^2) + \frac{E{\ell_1}^2}{1+\nu}({\eta_{xxx}}^2 + {\eta_{zzz}}^2 + 3{\eta_{xyy}}^2 + 3{\eta_{xzz}}^2 + 3{\eta_{zxx}}^2 + 3{\eta_{zyy}}^2) + \frac{E{\ell_2}^2}{1+\nu}\left(2{\chi_{xy}}^2 + 2{\chi_{yz}}^2\right) \right] dV \quad (11b)$$

where all components of strains in Eq. (11b) can be expressed via displacements and given in Appendix.

The potential energy (V) by the axial N_0 and uniformly load q(x):

$$V=-\frac{1}{2}\int_0^L N_0\left\{\left(\frac{\partial w_b}{\partial x}\right)^2+\left(\frac{\partial w_s}{\partial x}\right)^2+\left(\frac{\partial w_z}{\partial x}\right)^2+2\frac{\partial w_b}{\partial x}\frac{\partial w_s}{\partial x}+2\frac{\partial w_b}{\partial x}\frac{\partial w_z}{\partial x}++2\frac{\partial w_s}{\partial x}\frac{\partial w_z}{\partial x}\right\}dx-\int_0^L\{q(w_b+w_s+f_3(z)w_z\}dx \qquad (12)$$

The kinetic energy (K) is expressed with time (t) by:

$$K=\frac{1}{2}\int_V \rho(\dot{u}_1^2+\dot{u}_3^2)dV$$

$$=\frac{1}{2}\int_0^L\left[I_0\left\{\left(\frac{\partial u}{\partial t}\right)^2+\left(\frac{\partial w_b}{\partial t}\right)^2+\left(\frac{\partial w_s}{\partial t}\right)^2+2\left(\frac{\partial w_b}{\partial t}\right)\left(\frac{\partial w_s}{\partial t}\right)\right\}-2I_1\frac{\partial u}{\partial t}\frac{\partial^2 w_b}{\partial x\partial t}\right.$$
$$+I_2\left(\frac{\partial^2 w_b}{\partial x\partial t}\right)^2+2J_1\frac{\partial u}{\partial t}\frac{\partial^2 w_s}{\partial x\partial t}+2J_2\left\{\left(\frac{\partial w_b}{\partial t}\right)\left(\frac{\partial w_z}{\partial t}\right)+\left(\frac{\partial w_s}{\partial t}\right)\left(\frac{\partial w_z}{\partial t}\right)\right\}$$
$$-2J_3\frac{\partial^2 w_b}{\partial x\partial t}\frac{\partial^2 w_s}{\partial x\partial t}+K_1\left(\frac{\partial^2 w_s}{\partial x\partial t}\right)^2$$
$$\left.+K_2\left(\frac{\partial w_z}{\partial t}\right)^2\right]dx \qquad (13)$$

where the inertial coefficients are given by

$$(I_0,I_1,I_2,J_1,J_2,J_3,K_1,K_2)=\int_{-\frac{h}{2}}^{+\frac{h}{2}}\rho\left(1,f_1,{f_1}^2,f_2,f_3,f_1f_2,{f_2}^2,{f_3}^2\right)dz \qquad (14)$$

4. Finite Element Formulation

By using Hermite-cubic polynomial function, the displacement functions $u(x,t)$, $w_b(x,t)$, $w_s(x,t)$ and $w_z(x,t)$ can be expressed by using either two node beam element or three node beam element as follow.

4.1 Two node beam element (2NBE):

$$u(x,t)=\sum_{j=1}^{4}u_j\varphi_j(x)e^{i\omega t}, \qquad (15a)$$

$$w_b(x,t)=\sum_{j=1}^{4}{w_b}_j\varphi_j(x)e^{i\omega t}, \qquad (15b)$$

$$w_s(x,t) = \sum_{j=1}^{4} w_{s_j} \varphi_j(x) e^{i\omega t}, \tag{15c}$$

$$w_z(x,t) = \sum_{j=1}^{4} w_{z_j} \varphi_j(x) e^{i\omega t}, \tag{15d}$$

where ω is the natural frequency.

The unknows per element can be expressed in the form of:

$$u_j = \left[u^{(1)}, u_{,x}^{(1)}, u^{(2)}, u_{,x}^{(2)}\right] \tag{16a}$$

$$w_{b_j} = \left[w_b{}^{(1)}, w_{b}{}_{,x}^{(1)}, w_b{}^{(2)}, w_{b}{}_{,x}^{(2)}\right] \tag{16b}$$

$$w_{s_j} = \left[w_s{}^{(1)}, w_{s}{}_{,x}^{(1)}, w_s{}^{(2)}, w_{s}{}_{,x}^{(2)}\right] \tag{16c}$$

$$w_{z_j} = \left[w_z{}^{(1)}, w_{z}{}_{,x}^{(1)}, w_z{}^{(2)}, w_{z}{}_{,x}^{(2)}\right] \tag{16d}$$

Hermite interpolation functions can be given as follows:

$$\varphi_1(x) = 1 - \frac{3x^2}{l^2} + \frac{2x^3}{l^3} \tag{17a}$$

$$\varphi_2(x) = x - \frac{2x^2}{l} + \frac{x^3}{l^2} \tag{17b}$$

$$\varphi_3(x) = \frac{3x^2}{l^2} - \frac{2x^3}{l^3} \tag{17c}$$

$$\varphi_4(x) = -\frac{x^2}{l} + \frac{x^3}{l^2} \tag{17d}$$

4.2 Three node beam element (3NBE):

$$u(x,t) = \sum_{j=1}^{6} u_j \varphi_j(x) e^{i\omega t}, \tag{18a}$$

$$w_b(x,t) = \sum_{j=1}^{6} w_{b_j} \varphi_j(x) e^{i\omega t}, \tag{18b}$$

$$w_s(x,t) = \sum_{j=1}^{6} w_{s_j} \varphi_j(x) e^{i\omega t}, \tag{18c}$$

$$w_z(x,t) = \sum_{j=1}^{6} w_{z_j} \varphi_j(x) e^{i\omega t}, \tag{18d}$$

The unknows per element can be expressed in the form of:

$$u_j = \left[u^{(1)}, u_{,x}^{(1)}, u^{(2)}, u_{,x}^{(2)}, u^{(3)}, u_{,x}^{(3)}\right] \tag{19a}$$

$$w_{b_j} = \left[w_b{}^{(1)}, w_{b,x}^{(1)}, w_b{}^{(2)}, w_{b,x}^{(2)}, w_b{}^{(3)}, w_{b,x}^{(3)}\right] \tag{19b}$$

$$w_{s_j} = \left[w_s{}^{(1)}, w_{s,x}^{(1)}, w_s{}^{(2)}, w_{s,x}^{(2)}, w_s{}^{(3)}, w_{s,x}^{(3)}\right] \tag{19c}$$

$$w_{z_j} = \left[w_z{}^{(1)}, w_{z,x}^{(1)}, w_z{}^{(2)}, w_{z,x}^{(2)}, w_z{}^{(3)}, w_{z,x}^{(3)}\right] \tag{19d}$$

Hermite interpolation functions can be given as follows:

$$\varphi_1(x) = 1 - \frac{23x^2}{l^2} + \frac{66x^3}{l^3} - \frac{68x^4}{l^4} + \frac{24x^5}{l^5} \tag{20a}$$

$$\varphi_2(x) = x - \frac{6x^2}{l} + \frac{13x^3}{l^2} - \frac{12x^4}{l^3} + \frac{4x^5}{l^4} \tag{20b}$$

$$\varphi_3(x) = \frac{16x^2}{l^2} - \frac{32x^3}{l^3} + \frac{16x^4}{l^4} \tag{20c}$$

$$\varphi_4(x) = -\frac{8x^2}{l} + \frac{32x^3}{l^2} - \frac{40x^4}{l^3} + \frac{16x^5}{l^4} \tag{20d}$$

$$\varphi_5(x) = \frac{7x^2}{l^2} - \frac{34x^3}{l^3} + \frac{52x^4}{l^4} - \frac{24x^5}{l^5} \tag{20e}$$

$$\varphi_6(x) = -\frac{x^2}{l} + \frac{5x^3}{l^2} - \frac{8x^4}{l^3} + \frac{4x^5}{l^4} \tag{20f}$$

By using the Lagrange's equations and total energy (Π), the system of equations to be solved for unknown variables are obtained.

$$\Pi = U + V - K \tag{21a}$$

$$\frac{\partial \Pi}{\partial u_j} = 0, \quad \frac{\partial \Pi}{\partial w_{b_j}} = 0, \quad \frac{\partial \Pi}{\partial w_{s_j}} = 0, \quad \frac{\partial \Pi}{\partial w_{z_j}} = 0 \tag{21b}$$

By substituting Eq. (15) or Eq. (18) in to Eq. (21b), the system of equations can be expressed as the FEM of a typical element:

$$([K] - N_0[G] - \omega^2[M])\{\Delta\} = \{F\} \tag{22a}$$

$$\left(\begin{bmatrix} [K_{11}] & [K_{12}] & [K_{13}] & [K_{14}] \\ [K_{12}]^T & [K_{22}] & [K_{23}] & [K_{24}] \\ [K_{13}]^T & [K_{23}]^T & [K_{33}] & [K_{34}] \\ [K_{14}]^T & [K_{24}]^T & [K_{34}]^T & [K_{44}] \end{bmatrix} - N_0 \begin{bmatrix} [0] & [0] & [0] & [0] \\ [0]^T & [G_{22}] & [G_{23}] & [0] \\ [0]^T & [G_{23}]^T & [G_{33}] & [0] \\ [0]^T & [0]^T & [0]^T & [0] \end{bmatrix} - \omega^2 \begin{bmatrix} [M_{11}] & [M_{12}] & [M_{13}] & [0] \\ [M_{12}]^T & [M_{22}] & [M_{23}] & [M_{24}] \\ [M_{13}]^T & [M_{23}]^T & [M_{33}] & [M_{34}] \\ [M_{14}]^T & [M_{24}]^T & [M_{34}]^T & [M_{44}] \end{bmatrix}\right) \begin{Bmatrix} \{u_j\} \\ \{w_{b\,j}\} \\ \{w_{s\,j}\} \\ \{w_{z\,j}\} \end{Bmatrix} = \begin{Bmatrix} \{0\} \\ \{F_2\} \\ \{F_3\} \\ \{F_4\} \end{Bmatrix} \tag{22b}$$

where $\{\Delta\}$ is the nodal displacements, $[K_{kl}]$, $[M_{kl}]$ and $[G_{kl}]$ are the stiffness, mass and geometric stiffness matrices and F_k is the nodal force vector, respectively. Their components and the equations of motion are given in Appendix. The displacements, frequencies and buckling loads can be found by solving Eq. (22).

5. Numerical Examples

In this section, the size-dependent responses of 2D FG porous microbeams with respect to porosity coefficients (α_0), variable MLSP (ℓ), and gradient indices (p_x, p_z), as well as boundary conditions (BCs) are studied. The kinematic boundary conditions are given in Table 1. They are made of Al and SiC with material properties given by (Al: $E_m = 70\ GPa$, $\nu_m = 0.3$, $\rho_m = 2702\ kg/m^3, \ell_m = 15\ \mu m$; SiC: $E_c = 427\ GPa$, $\nu_c = 0.17$, $\rho_c = 3100\ kg/m^3, \ell_c = 22.5\ \mu m$. Three MLSPs are assumed to be the same value $\ell = \ell_0 = \ell_1 = \ell_2$. The dimensionless fundamental frequency (DFF) (λ), critical buckling load (DCBL) (N_{cr}) and mid-span deflection (DMD) ($\overline{w}$) are defined as below:

$$\lambda = \frac{\omega L^2}{h}\sqrt{\frac{\rho_m}{E_m}} \tag{23a}$$

$$N_{cr} = N_0 \frac{12L^2}{E_c h^3} \tag{23b}$$

$$\overline{w} = w \frac{10^3 E_m h^3}{qL^4} \tag{23c}$$

5.1 2D FG microbeams

Since there are no available results for the present model (Q3D and MGST), verification is carried out for 2D FG microbeams using a TBT and the MCST. It should be noted that the results of the MCST, which is special case of the MSGT, can be obtained by assigning $\ell_0 = \ell_1 = 0$. For convergence study, various number of elements are used to compare the obtained results from 2NBE and 3NBE with those presented by Chen et al. [54] using differential quadrature method (DQM) in Table 2. There is a negligible difference between the results of 2NBE and 3NBE. Table 2 verifies that the FEM has converged to a solution and 70 elements can produce satisfactory numerical results with those from previous study [54]. Therefore, 70 elements of 2NBE are used for the numerical examples in the following examples.

The frequencies and buckling loads for S-S and C-C beams for various gradient index are given in Tables 3 and 4 and compared with previous results [54]. There is the slightly difference between the present results and those from previous study, which neglected normal strain effect. These tables clearly show that the accuracy of the proposed theory. The displacements from the MCST and all results from the MSGT for various BCs are also given in Tables 5 and 6. The results predicted by variable MLSP, which is the position-dependent model, are notablely different from those evaluated by constant one. The inclusion of variable MLSP leads to increase frequencies and buckling loads and decrease displacements.

Ratios of DMDs, DFFs and DCBLs of S-S 2D FG microbeams between the results obtained from variable MLSP and constant one with respect to p_x and p_z is given in Fig. 3. As expected, the ratios of buckling and frequencies are greater than one and those of displacements are less than that. It is clear that the effect of variable MLSP is more pronounced for very small beam $(h/\ell_m = 1)$ and small gradient indices. As gradient indices increase and larger than 5, these ratios become flat and effect of variable MLSP is negligible. It has the strongest influence for C-C beam and weakest for C-F one as shown in Fig. 4. It is interesting to observe that even for $h/\ell_m = 1$, when $p_z = 1$, as p_x increases, three ratios reach to unity when $p_x = 5$ and 10 for C-F and S-S beam. Figs. 3 and 4 also show that effect of gradient index in axial direction on variable MLSP is more significant than thickness direction.

5.2 2D FG porous microbeams

As shown in Tables 7 and 8, the frequencies and buckling loads of 2D FGM I and II porous microbeams show good agreement with previous ones [47, 48, 53], which again demonstrates the validation of the present theory. The reference MCST results were obtained from the CBT/FBT [47, 48] using generalized DQM and a Q3D TBT [53] using FEM. New results from the MCST/MSGT with constant and variable MLSP for simply supported boundary conditions are also given in Tables 9-11 as a benchmark for future studies. It can be observed again that the results obtained from latter are significantly different from those from former. The buckling loads and frequencies become larger, contrarily the displacements become less.

The variation of DMDs, DFFs, and DCBLs of C-C 2D perfect and imperfect FG microbeams is plotted in Fig. 5. Among them, the DMDs of perfect FG microbeams are the smallest and those of 2D FGM I are the largest. The increment of α_0, p_x and p_z decreases the buckling load, frequencies and increases displacements (Fig. 5). It can be observed that the gradient indices p_x and p_z have strong effect on the results when they are less than 5.

Two types of ratios, the first one from the results of the MGST to MCST and second one from those from variable MLSP to constant one, for various BCs are plotted in Fig. 6. It can be seen that there is slightly different in the first ratio among three BCs (Fig. 6a), whereas significant difference for second one (Fig. 6b) especially when beam's thickness is very small ($h/\ell_m = 1$). At this scale, for C-C beams, the first and second ratios of DCBLs are appoximately 2.4 and 1.23. As (h/ℓ_m) increases, the first and second ratio approach unity as $h/\ell_m = 20$ and 30. It implies that the MSGT with three variable MLSPs should be considered for better results in the range of $h/\ell_m \in [1,20]$. From that point, MCST with one MLSP can be used from $h/\ell_m \in [20,30]$.

5.3 Effect of variable length scale parameter

The variations of DMDs, DFFs and DCBLs of 2D perfect and imperfect FG microbeams with respect to (h/ℓ_m) are plotted in Fig. 7 with four different values of (ℓ_m/ℓ_c). It should be noted that MLSP is constant only when $\ell_m = \ell_c$ and the rest are variable MLSP. As (ℓ_m/ℓ_c) changes from 1/2 to 2, DFFs and DCBLs increase and DMDs decrease. The increase is significant when (h/ℓ_m) is relatively small and negligible as (h/ℓ_m) as large as 15 for DCBLs and DFFs. Besides, it is more noticeable for DMDs compared to other responses. This confirms again that variable MLSP should be included in analysis of 2D FG microbeams.

6. Conclusion

A quasi-3D theory based on the MSGT with three variable MLSPs for 2D FG porous microbeams is presented. The governing equations for static, vibration and buckling analysis are derived by using the Lagrange's equations and solved by beam element. Two porosity models including even and uneven are considered to investigate the effects of variable MLSP, porosity distribution, gradient index in both axial and thickness directions, as well as boundary conditions on the structural responses of 2D FG porous microbeams. The results indicate these mentioned effects have significant influence on the structural responses of microbeams. The main results of this paper are included below:

- ✓ As the MSGT includes three MLSPs, the results from this theory is more accurate than those from the MCST and classical theory especially when h/l_m approaches to 1.
- ✓ The even distributions of porosities (FGM I) lead to lower natural frequencies, buckling loads as well as higher displacements rather than uneven one (FGM II).

- ✓ The inclusion of variable MLSP leads to increase frequencies and buckling loads and decrease displacements.
- ✓ The variation of MLSP should be considered in the analysis of 2D FG porous microbeams.

References

[1] D. Hasanyan, R. Batra, S. Harutyunyan, Pull-In Instabilities in Functionally Graded Microthermoelectromechanical Systems, Journal Of Thermal Stresses. 31 (2008) 1006-1021. doi:10.1080/01495730802250714.

[2] B. Mohammadi-Alasti, G. Rezazadeh, A. Borgheei, S. Minaei, R. Habibifar, On the mechanical behavior of a functionally graded micro-beam subjected to a thermal moment and nonlinear electrostatic pressure, Composite Structures. 93 (2011) 1516-1525. doi:10.1016/j.compstruct.2010.11.013.

[3] Y. Fu, H. Du, S. Zhang, Functionally graded TiN/TiNi shape memory alloy films, Materials Letters. 57 (2003) 2995-2999. doi:10.1016/s0167-577x(02)01419-2.

[4] A. Witvrouw, A. Mehta, The Use of Functionally Graded Poly-SiGe Layers for MEMS Applications, Materials Science Forum. 492-493 (2005) 255-260. doi:10.4028/www.scientific.net/msf.492-493.255.

[5] C. Lü, C. Lim, W. Chen, Size-dependent elastic behavior of FGM ultra-thin films based on generalized refined theory, International Journal Of Solids And Structures. 46 (2009) 1176-1185. doi:10.1016/j.ijsolstr.2008.10.012.

[6] M. Rahaeifard, M.M. Kahrobaiyan, M.T. Ahmadian, Sensitivity Analysis of Atomic Force Microscope Cantilever Made of Functionally Graded Materials, Proceedings of the ASME 2009 International Design Engineering Technical Conferences and Computers and Information in Engineering Conference. Volume 6: ASME Power Transmission and Gearing Conference; 3rd International Conference on Micro- and Nanosystems; 11th International Conference on Advanced Vehicle and Tire *Technologies*. San Diego, California, (2009) 539-544. https://doi.org/10.1115/DETC2009-86254

[7] R. Toupin, Elastic materials with couple-stresses, Archive For Rational Mechanics And Analysis. 11 (1962) 385-414. doi:10.1007/bf00253945.

[8] R. Mindlin, H. Tiersten, Effects of couple-stresses in linear elasticity, Archive For Rational Mechanics And Analysis. 11 (1962) 415-448. doi:10.1007/bf00253946.

[9] N. Fleck, J. Hutchinson, A phenomenological theory for strain gradient effects in plasticity, Journal Of The Mechanics And Physics Of Solids. 41 (1993) 1825-1857. doi:10.1016/0022-5096(93)90072-n.

[10] F. Yang, A. Chong, D. Lam, P. Tong, Couple stress based strain gradient theory for elasticity, International Journal Of Solids And Structures. 39 (2002) 2731-2743. doi:10.1016/s0020-7683(02)00152-x.

[11] D. Lam, F. Yang, A. Chong, J. Wang, P. Tong, Experiments and theory in strain gradient elasticity, Journal Of The Mechanics And Physics Of Solids. 51 (2003) 1477-1508. doi:10.1016/s0022-5096(03)00053-x.

[12] A. Eringen, Linear theory of micropolar elasticity, *Journal of Mathematics and Mechanics*, 15(6) (1966) 909-923.

[13] A. Eringen, Nonlocal polar elastic continua, International Journal Of Engineering Science. 10 (1972) 1-16. doi:10.1016/0020-7225(72)90070-5.

[14] S. Kong, S. Zhou, Z. Nie, K. Wang, Static and dynamic analysis of micro beams based on strain gradient elasticity theory, International Journal Of Engineering Science. 47 (2009) 487-498. doi:10.1016/j.ijengsci.2008.08.008.

[15] B. Akgöz, Ö. Civalek, Strain gradient elasticity and modified couple stress models for buckling analysis of axially loaded micro-scaled beams, International Journal Of Engineering Science. 49 (2011) 1268-1280. doi:10.1016/j.ijengsci.2010.12.009.

[16] B. Akgöz, Ö. Civalek, Longitudinal vibration analysis of strain gradient bars made of functionally graded materials (FGM), Composites Part B: Engineering. 55 (2013) 263-268. doi:10.1016/j.compositesb.2013.06.035.

[17] B. Akgöz, Ö. Civalek, Buckling analysis of functionally graded microbeams based on the strain gradient theory, Acta Mechanica. 224 (2013) 2185-2201. doi:10.1007/s00707-013-0883-5.

[18] M. Rahaeifard, M. Kahrobaiyan, M. Ahmadian, K. Firoozbakhsh, Strain gradient formulation of functionally graded nonlinear beams, International Journal Of Engineering Science. 65 (2013) 49-63. doi:10.1016/j.ijengsci.2013.02.002.

[19] R. Ansari, R. Gholami, S. Sahmani, Free vibration analysis of size-dependent functionally graded microbeams based on the strain gradient Timoshenko beam theory, Composite Structures. 94 (2011) 221-228. doi:10.1016/j.compstruct.2011.06.024.

[20] S. Tajalli, M. Rahaeifard, M. Kahrobaiyan, M. Movahhedy, J. Akbari, M. Ahmadian, Mechanical behavior analysis of size-dependent micro-scaled functionally graded Timoshenko beams by strain gradient elasticity theory, Composite Structures. 102 (2013) 72-80. doi:10.1016/j.compstruct.2013.03.001.

[21] R. Ansari, R. Gholami, M. Faghih Shojaei, V. Mohammadi, S. Sahmani, Size-dependent bending, buckling and free vibration of functionally graded Timoshenko microbeams based on the most general strain gradient theory, Composite Structures. 100 (2013) 385-397. doi:10.1016/j.compstruct.2012.12.048.

[22] B. Zhang, Y. He, D. Liu, Z. Gan, L. Shen, Non-classical Timoshenko beam element based on the strain gradient elasticity theory, Finite Elements In Analysis And Design. 79 (2014) 22-39. doi:10.1016/j.finel.2013.10.004.

[23] B. Akgöz, Ö. Civalek, Shear deformation beam models for functionally graded microbeams with new shear correction factors, Composite Structures. 112 (2014) 214-225. doi:10.1016/j.compstruct.2014.02.022.

[24] B. Zhang, Y. He, D. Liu, Z. Gan, L. Shen, Size-dependent functionally graded beam model based on an improved third-order shear deformation theory, European Journal Of Mechanics - A/Solids. 47 (2014) 211-230. doi:10.1016/j.euromechsol.2014.04.009.

[25] S. Sahmani, M. Bahrami, R. Ansari, Nonlinear free vibration analysis of functionally graded third-order shear deformable microbeams based on the modified strain gradient elasticity theory, Composite Structures. 110 (2014) 219-230. doi:10.1016/j.compstruct.2013.12.004.

[26] S. Sahmani, R. Ansari, Size-dependent buckling analysis of functionally graded third-order shear deformable microbeams including thermal environment effect, Applied Mathematical Modelling. 37 (2013) 9499-9515. doi:10.1016/j.apm.2013.04.051.

[27] A. Karamanli, T. Vo, Size-dependent behaviour of functionally graded sandwich microbeams based on the modified strain gradient theory, Composite Structures. 246 (2020) 112401. doi:10.1016/j.compstruct.2020.112401.

[28] J. Lei, Y. He, B. Zhang, Z. Gan, P. Zeng, Bending and vibration of functionally graded sinusoidal microbeams based on the strain gradient elasticity theory, International Journal Of Engineering Science. 72 (2013) 36-52. doi:10.1016/j.ijengsci.2013.06.012.

[29] B. Akgöz, Ö. Civalek, A size-dependent shear deformation beam model based on the strain gradient elasticity theory, International Journal Of Engineering Science. 70 (2013) 1-14. doi:10.1016/j.ijengsci.2013.04.004.

[30] B. Akgöz, Ö. Civalek, A new trigonometric beam model for buckling of strain gradient microbeams, International Journal Of Mechanical Sciences. 81 (2014) 88-94. doi:10.1016/j.ijmecsci.2014.02.013.

[31] B. Akgöz, Ö. Civalek, A novel microstructure-dependent shear deformable beam model, International Journal Of Mechanical Sciences. 99 (2015) 10-20. doi:10.1016/j.ijmecsci.2015.05.003.

[32] H. Thai, T. Vo, T. Nguyen, S. Kim, A review of continuum mechanics models for size-dependent analysis of beams and plates, Composite Structures. 177 (2017) 196-219. doi:10.1016/j.compstruct.2017.06.040.

[33] M. Ghayesh, A. Farajpour, A review on the mechanics of functionally graded nanoscale and microscale structures, International Journal Of Engineering Science. 137 (2019) 8-36. doi:10.1016/j.ijengsci.2018.12.001.

[34] F.R. Hall, D.R. Hayhurst. Modelling of grain size effects in creep crack growth using a non-local continuum damage. Proceedings: Mathematical and Physical Sciences 433(1888) (1991) 405-421.

[35] W. Sumelka. On fractional non-local bodies with variable length scale, Mechanics Research Communications, 86, 2017, 5-10

[36] R.H.J. Peerlings, M.G.D. Geers, R. de Borst, W.A.M. Brekelmans, A critical comparison of nonlocal and gradient-enhanced softening continua, International Journal of Solids and Structures, 38(44–45), 2001, 7723-7746.

[37] P. Stempin, W. Sumelka. Space-fractional Euler-Bernoulli beam model - Theory and identification for silver nanobeam bending, International Journal of Mechanical Sciences, 186, 2020, 105902

[38] W. Nix, H. Gao, Indentation size effects in crystalline materials: A law for strain gradient plasticity, Journal Of The Mechanics And Physics Of Solids. 46 (1998) 411-425. doi:10.1016/s0022-5096(97)00086-0.

[39] M. Kahrobaiyan, M. Rahaeifard, S. Tajalli, M. Ahmadian, A strain gradient functionally graded Euler–Bernoulli beam formulation, International Journal Of Engineering Science. 52 (2012) 65-76. doi:10.1016/j.ijengsci.2011.11.010.

[40] R. Aghazadeh, E. Cigeroglu, S. Dag, Static and free vibration analyses of small-scale functionally graded beams possessing a variable length scale parameter using different beam theories, European Journal Of Mechanics - A/Solids. 46 (2014) 1-11. doi:10.1016/j.euromechsol.2014.01.002.

[41] K. Al-Basyouni, A. Tounsi, S. Mahmoud, Size dependent bending and vibration analysis of functionally graded micro beams based on modified couple stress theory and neutral surface position, Composite Structures. 125 (2015) 621-630. doi:10.1016/j.compstruct.2014.12.070.

[42] A. Babaei, M. Noorani, A. Ghanbari, Temperature-dependent free vibration analysis of functionally graded micro-beams based on the modified couple stress theory, Microsystem Technologies. 23 (2017) 4599-4610. doi:10.1007/s00542-017-3285-0.

[43] A. Babaei, A. Rahmani, On dynamic-vibration analysis of temperature-dependent Timoshenko microbeam possessing mutable nonclassical length scale parameter, Mechanics Of Advanced Materials And Structures. (2018) 1-8. doi:10.1080/15376494.2018.1516252.

[44] M. Nemat-Alla, Reduction of thermal stresses by developing two-dimensional functionally graded materials, International Journal Of Solids And Structures. 40 (2003) 7339-7356. doi:10.1016/j.ijsolstr.2003.08.017.

[45] N. Wattanasakulpong, B. Gangadhara Prusty, D. Kelly, M. Hoffman, Free vibration analysis of layered functionally graded beams with experimental validation, Materials & Design (1980-2015). 36 (2012) 182-190. doi:10.1016/j.matdes.2011.10.049.

[46] J. Zhu, Z. Lai, Z. Yin, J. Jeon, S. Lee, Fabrication of ZrO2–NiCr functionally graded material by powder metallurgy, Materials Chemistry And Physics. 68 (2001) 130-135. doi:10.1016/s0254-0584(00)00355-2.

[47] N. Shafiei, S. Mirjavadi, B. MohaselAfshari, S. Rabby, M. Kazemi, Vibration of two-dimensional imperfect functionally graded (2D-FG) porous nano-/micro-beams, Computer Methods In Applied Mechanics And Engineering. 322 (2017) 615-632. doi:10.1016/j.cma.2017.05.007.

[48] N. Shafiei, M. Kazemi, Buckling analysis on the bi-dimensional functionally graded porous tapered nano-/micro-scale beams, Aerospace Science And Technology. 66 (2017) 1-11. doi:10.1016/j.ast.2017.02.019.

[49] L. Trinh, T. Vo, H. Thai, T. Nguyen, Size-dependent vibration of bi-directional functionally graded microbeams with arbitrary boundary conditions, Composites Part B: Engineering. 134 (2018) 225-245. doi:10.1016/j.compositesb.2017.09.054.

[50] T. Yu, J. Zhang, H. Hu, T. Bui, A novel size-dependent quasi-3D isogeometric beam model for two-directional FG microbeams analysis, Composite Structures. 211 (2019) 76-88. doi:10.1016/j.compstruct.2018.12.014.

[51] A. Karamanlı, T. Vo, Size dependent bending analysis of two directional functionally graded microbeams via a quasi-3D theory and finite element method, Composites Part B: Engineering. 144 (2018) 171-183. doi:10.1016/j.compositesb.2018.02.030.

[52] A. Karamanli, M. Aydogdu, Size dependent flapwise vibration analysis of rotating two-directional functionally graded sandwich porous microbeams based on a transverse shear and normal deformation theory, International Journal Of Mechanical Sciences. 159 (2019) 165-181. doi:10.1016/j.ijmecsci.2019.05.047.

[53] A. Karamanli, M. Aydogdu, Structural dynamics and stability analysis of 2D-FG microbeams with two-directional porosity distribution and variable material length scale parameter, Mechanics Based Design Of Structures And Machines. 48 (2019) 164-191. doi:10.1080/15397734.2019.1627219.

[54] X. Chen, Y. Lu, Y. Li, Free vibration, buckling and dynamic stability of bi-directional FG microbeam with a variable length scale parameter embedded in elastic medium, Applied Mathematical Modelling. 67 (2019) 430-448. doi:10.1016/j.apm.2018.11.004.

[55] X. Chen, X. Zhang, Y. Lu, Y. Li, Static and dynamic analysis of the postbuckling of bi-directional functionally graded material microbeams, International Journal Of Mechanical Sciences. 151 (2019) 424-443. doi:10.1016/j.ijmecsci.2018.12.001.

[56] N. Wattanasakulpong, A. Chaikittiratana, Flexural vibration of imperfect functionally graded beams based on Timoshenko beam theory: Chebyshev collocation method, Meccanica. 50 (2015) 1331-1342. doi:10.1007/s11012-014-0094-8.

[57] N. Shafiei, A. Mousavi & M. Ghadiri. On size-dependent nonlinear vibration of porous and imperfect functionally graded tapered microbeams, International Journal of Engineering Science, 2016, 106, 42 – 56.

Appendix

1. Strain components in Eq. (11) are given by:

$$\varepsilon_x{}^2 = \left(\frac{\partial u}{\partial x}\right)^2 + f_1{}^2\left(\frac{\partial^2 w_b}{\partial x^2}\right)^2 + f_2{}^2\left(\frac{\partial^2 w_s}{\partial x^2}\right)^2 - 2f_1\left(\frac{\partial u}{\partial x}\right)\left(\frac{\partial^2 w_b}{\partial x^2}\right) + 2f_2\left(\frac{\partial u}{\partial x}\right)\left(\frac{\partial^2 w_s}{\partial x^2}\right) - 2f_1 f_2\left(\frac{\partial^2 w_b}{\partial x^2}\right)\left(\frac{\partial^2 w_s}{\partial x^2}\right) \quad (A1a)$$

$$\varepsilon_x\varepsilon_z = f_3{}'\left(\frac{\partial u}{\partial x}\right)w_z - f_3{}' f_1\left(\frac{\partial^2 w_b}{\partial x^2}\right)w_z + f_3{}' f_2\left(\frac{\partial^2 w_s}{\partial x^2}\right)w_z \quad (A1b)$$

$$\varepsilon_z{}^2 = (f_3{}')^2 w_z{}^2 \quad (A1c)$$

$$\gamma_{xz}{}^2 = (f_3)^2\left[\left(\frac{\partial w_b}{\partial x}\right)^2 + 4\left(\frac{\partial w_s}{\partial x}\right)^2 + \left(\frac{\partial w_z}{\partial x}\right)^2 + 4\left(\frac{\partial w_b}{\partial x}\right)\left(\frac{\partial w_s}{\partial x}\right) + 2\left(\frac{\partial w_b}{\partial x}\right)\left(\frac{\partial w_z}{\partial x}\right) + 4\left(\frac{\partial w_s}{\partial x}\right)\left(\frac{\partial w_z}{\partial x}\right)\right] \quad (A1d)$$

$$\chi_{xy}{}^2 = \frac{1}{16}\left[\left(1+\frac{df_1}{dz}\right)^2\left(\frac{d^2 w_b}{dx^2}\right)^2 + \left(1-\frac{df_2}{dz}\right)^2\left(\frac{d^2 w_s}{dx^2}\right)^2 + f_3{}^2\left(\frac{d^2 w_z}{dx^2}\right)^2 + 2\left(1+\frac{df_1}{dz}\right)\left(1-\frac{df_2}{dz}\right)\left(\frac{d^2 w_b}{dx^2}\right)\left(\frac{d^2 w_s}{dx^2}\right) + 2\left(1+\frac{df_1}{dz}\right)f_3\left(\frac{d^2 w_b}{dx^2}\right)\left(\frac{d^2 w_z}{dx^2}\right) + 2\left(1-\frac{df_2}{dz}\right)f_3\left(\frac{d^2 w_s}{dx^2}\right)\left(\frac{d^2 w_z}{dx^2}\right)\right] \quad (A1e)$$

$$\chi_{yz}{}^2 = \frac{1}{16}\left[\left(\frac{d^2 f_1}{dz^2}\right)^2\left(\frac{dw_b}{dx}\right)^2 + \left(\frac{d^2 f_2}{dz^2}\right)^2\left(\frac{dw_s}{dx}\right)^2 + \left(\frac{df_3}{dz}\right)^2\left(\frac{dw_z}{dx}\right)^2 - 2\left(\frac{d^2 f_1}{dz^2}\right)\left(\frac{d^2 f_2}{dz^2}\right)\left(\frac{dw_b}{dx}\right)\left(\frac{dw_s}{dx}\right) + 2\left(\frac{d^2 f_1}{dz^2}\right)\left(\frac{df_3}{dz}\right)\left(\frac{dw_b}{dx}\right)\left(\frac{dw_z}{dx}\right) - 2\left(\frac{d^2 f_2}{dz^2}\right)\left(\frac{df_3}{dz}\right)\left(\frac{dw_s}{dx}\right)\left(\frac{dw_z}{dx}\right)\right] \quad (A1f)$$

$$\gamma_x{}^2 = \left(\frac{d^2u}{dx^2}\right)^2 + f_1{}^2\left(\frac{d^3w_b}{dx^3}\right)^2 + f_2{}^2\left(\frac{d^3w_s}{dx^3}\right)^2 + \left(\frac{df_3}{dz}\right)^2\left(\frac{dw_z}{dx}\right)^2 - 2f_1\left(\frac{d^2u}{dx^2}\right)\left(\frac{d^3w_b}{dx^3}\right)$$

$$+ 2f_2\left(\frac{d^2u}{dx^2}\right)\left(\frac{d^3w_s}{dx^3}\right) + 2\left(\frac{df_3}{dz}\right)\left(\frac{d^2u}{dx^2}\right)\left(\frac{dw_z}{dx}\right) - 2f_1f_2\left(\frac{d^3w_b}{dx^3}\right)\left(\frac{d^3w_s}{dx^3}\right)$$

$$- 2f_1\left(\frac{df_3}{dz}\right)\left(\frac{d^3w_b}{dx^3}\right)\left(\frac{dw_z}{dx}\right) + 2f_2\left(\frac{df_3}{dz}\right)\left(\frac{d^3w_s}{dx^3}\right)\left(\frac{dw_z}{dx}\right) \qquad (A1g)$$

$$\gamma_z{}^2 = \left(\frac{df_1}{dz}\right)^2\left(\frac{d^2w_b}{dx^2}\right)^2 + \left(\frac{df_2}{dz}\right)^2\left(\frac{d^2w_s}{dx^2}\right)^2 + \left(\frac{d^2f_3}{dz^2}\right)^2 w_z{}^2 - 2\left(\frac{df_1}{dz}\right)\left(\frac{df_2}{dz}\right)\left(\frac{d^2w_b}{dx^2}\right)\left(\frac{d^2w_s}{dx^2}\right)$$

$$- 2\left(\frac{df_1}{dz}\right)\left(\frac{d^2f_3}{dz^2}\right)\left(\frac{d^2w_b}{dx^2}\right)w_z + 2\left(\frac{df_2}{dz}\right)\left(\frac{d^2f_3}{dz^2}\right)\left(\frac{d^2w_s}{dx^2}\right)w_z \qquad (A1h)$$

$$\eta_{xxx}{}^2 = \frac{1}{25}\Bigg[4\left(\frac{d^2u}{dx^2}\right)^2 - 8f_1\left(\frac{d^2u}{dx^2}\right)\left(\frac{d^3w_b}{dx^3}\right) - 4\left(\frac{df_3}{dz}\right)\left(\frac{d^2u}{dx^2}\right)\left(\frac{dw_b}{dx}\right) + 8f_2\left(\frac{d^2u}{dx^2}\right)\left(\frac{d^3w_s}{dx^3}\right)$$

$$- 8\left(\frac{df_3}{dz}\right)\left(\frac{d^2u}{dx^2}\right)\left(\frac{dw_s}{dx}\right) - 8\left(\frac{df_3}{dz}\right)\left(\frac{d^2u}{dx^2}\right)\left(\frac{dw_z}{dx}\right) + 4f_1{}^2\left(\frac{d^3w_b}{dx^3}\right)^2$$

$$+ \left(\frac{df_3}{dz}\right)^2\left(\frac{dw_b}{dx}\right)^2 + 4f_1\left(\frac{df_3}{dz}\right)\left(\frac{d^3w_b}{dx^3}\right)\left(\frac{dw_b}{dx}\right) - 8f_1f_2\left(\frac{d^3w_b}{dx^3}\right)\left(\frac{d^3w_s}{dx^3}\right)$$

$$+ 8f_1\left(\frac{df_3}{dz}\right)\left(\frac{d^3w_b}{dx^3}\right)\left(\frac{dw_s}{dx}\right) - 4f_2\left(\frac{df_3}{dz}\right)\left(\frac{dw_b}{dx}\right)\left(\frac{d^3w_s}{dx^3}\right) + 4\left(\frac{df_3}{dz}\right)^2\left(\frac{dw_b}{dx}\right)\left(\frac{dw_s}{dx}\right)$$

$$+ 4\left(\frac{df_3}{dz}\right)^2\left(\frac{dw_b}{dx}\right)\left(\frac{dw_z}{dx}\right) + 8f_1\left(\frac{df_3}{dz}\right)\left(\frac{d^3w_b}{dx^3}\right)\left(\frac{dw_z}{dx}\right) + 4f_2{}^2\left(\frac{d^3w_s}{dx^3}\right)^2$$

$$+ 4\left(\frac{df_3}{dz}\right)^2\left(\frac{dw_s}{dx}\right)^2 - 8f_2\left(\frac{df_3}{dz}\right)\left(\frac{d^3w_s}{dx^3}\right)\left(\frac{dw_s}{dx}\right) - 8f_2\left(\frac{df_3}{dz}\right)\left(\frac{d^3w_s}{dx^3}\right)\left(\frac{dw_z}{dx}\right)$$

$$+ 8\left(\frac{df_3}{dz}\right)^2\left(\frac{dw_s}{dx}\right)\left(\frac{dw_z}{dx}\right) + 4\left(\frac{df_3}{dz}\right)^2\left(\frac{dw_z}{dx}\right)^2\Bigg] \qquad (A1i)$$

$$
\begin{aligned}
{\eta_{zzz}}^2 = \frac{1}{25}\Bigg[& \left(\frac{df_1}{dz}\right)^2 \left(\frac{d^2w_b}{dx^2}\right)^2 - 2\left(\frac{df_1}{dz}\right) f_3 \left(\frac{d^2w_b}{dx^2}\right)^2 + (f_3)^2 \left(\frac{d^2w_b}{dx^2}\right)^2 \\
& - 2\left(\frac{df_1}{dz}\right)\left(\frac{df_2}{dz}\right)\left(\frac{d^2w_b}{dx^2}\right)\left(\frac{d^2w_s}{dx^2}\right) - 4\left(\frac{df_1}{dz}\right)(f_3)\left(\frac{d^2w_b}{dx^2}\right)\left(\frac{d^2w_s}{dx^2}\right) \\
& + 2\left(\frac{df_2}{dz}\right)(f_3)\left(\frac{d^2w_b}{dx^2}\right)\left(\frac{d^2w_s}{dx^2}\right) + 4(f_3)^2\left(\frac{d^2w_b}{dx^2}\right)\left(\frac{d^2w_s}{dx^2}\right) \\
& - 2\left(\frac{df_1}{dz}\right)(f_3)\left(\frac{d^2w_b}{dx^2}\right)\left(\frac{d^2w_z}{dx^2}\right) + 2(f_3)^2 \left(\frac{d^2w_b}{dx^2}\right)\left(\frac{d^2w_z}{dx^2}\right) \\
& + 4\left(\frac{df_1}{dz}\right)\left(\frac{d^2f_3}{dz^2}\right)\left(\frac{d^2w_b}{dx^2}\right) w_z - 4(f_3)\left(\frac{d^2f_3}{dz^2}\right)\left(\frac{d^2w_b}{dx^2}\right) w_z + \left(\frac{df_2}{dz}\right)^2 \left(\frac{d^2w_s}{dx^2}\right)^2 \\
& + 4\left(\frac{df_2}{dz}\right)(f_3)\left(\frac{d^2w_s}{dx^2}\right)^2 + 4(f_3)^2\left(\frac{d^2w_s}{dx^2}\right)^2 + 2\left(\frac{df_2}{dz}\right)(f_3)\left(\frac{d^2w_s}{dx^2}\right)\left(\frac{d^2w_z}{dx^2}\right) \\
& + 4(f_3)^2\left(\frac{d^2w_s}{dx^2}\right)\left(\frac{d^2w_z}{dx^2}\right) - 4\left(\frac{df_2}{dz}\right)\left(\frac{d^2f_3}{dz^2}\right)\left(\frac{d^2w_s}{dx^2}\right) w_z \\
& - 8(f_3)\left(\frac{d^2f_3}{dz^2}\right)\left(\frac{d^2w_s}{dx^2}\right) w_z + (f_3)^2\left(\frac{d^2w_z}{dx^2}\right)^2 \\
& + 4\left(\frac{d^2f_3}{dz^2}\right)^2 {w_z}^2 - 4(f_3)\left(\frac{d^2f_3}{dz^2}\right) w_z \left(\frac{d^2w_z}{dx^2}\right)\Bigg] \qquad (A1j)
\end{aligned}
$$

$$3{\eta_{xyy}}^2 = \frac{3}{225}\left[9\left(\frac{d^2u}{dx^2}\right)^2 + 6\left(\frac{df_3}{dz}\right)\left(\frac{d^2u}{dx^2}\right)\left(\frac{dw_b}{dx}\right) - 18f_1\left(\frac{d^2u}{dx^2}\right)\left(\frac{d^3w_b}{dx^3}\right)\right.$$

$$+ 12\left(\frac{df_3}{dz}\right)\left(\frac{d^2u}{dx^2}\right)\left(\frac{dw_s}{dx}\right) + 18f_2\left(\frac{d^2u}{dx^2}\right)\left(\frac{d^3w_s}{dx^3}\right) + 12\left(\frac{df_3}{dz}\right)\left(\frac{d^2u}{dx^2}\right)\left(\frac{dw_z}{dx}\right)$$

$$+ 9{f_1}^2\left(\frac{d^3w_b}{dx^3}\right)^2 - 6f_1\left(\frac{df_3}{dz}\right)\left(\frac{d^3w_b}{dx^3}\right)\left(\frac{dw_b}{dx}\right) + \left(\frac{df_3}{dz}\right)^2\left(\frac{dw_b}{dx}\right)^2$$

$$- 18f_1f_2\left(\frac{d^3w_b}{dx^3}\right)\left(\frac{d^3w_s}{dx^3}\right) - 12f_1\left(\frac{df_3}{dz}\right)\left(\frac{d^3w_b}{dx^3}\right)\left(\frac{dw_s}{dx}\right)$$

$$+ 6f_2\left(\frac{df_3}{dz}\right)\left(\frac{dw_b}{dx}\right)\left(\frac{d^3w_s}{dx^3}\right) + 4\left(\frac{df_3}{dz}\right)^2\left(\frac{dw_b}{dx}\right)\left(\frac{dw_s}{dx}\right)$$

$$- 12f_1\left(\frac{df_3}{dz}\right)\left(\frac{d^3w_b}{dx^3}\right)\left(\frac{dw_z}{dx}\right) + 4\left(\frac{df_3}{dz}\right)^2\left(\frac{dw_b}{dx}\right)\left(\frac{dw_z}{dx}\right) + 9{f_2}^2\left(\frac{d^3w_s}{dx^3}\right)^2$$

$$+ 4\left(\frac{df_3}{dz}\right)^2\left(\frac{dw_s}{dx}\right)^2 + 12f_2\left(\frac{df_3}{dz}\right)\left(\frac{d^3w_s}{dx^3}\right)\left(\frac{dw_s}{dx}\right)$$

$$\left. + 12f_2\left(\frac{df_3}{dz}\right)\left(\frac{d^3w_s}{dx^3}\right)\left(\frac{dw_z}{dx}\right) + 8\left(\frac{df_3}{dz}\right)^2\left(\frac{dw_s}{dx}\right)\left(\frac{dw_z}{dx}\right) + 4\left(\frac{df_3}{dz}\right)^2\left(\frac{dw_z}{dx}\right)^2\right] \quad (A1k)$$

$$
\begin{aligned}
3{\eta_{xzz}}^2 = \frac{3}{225}\Bigg[&9\left(\frac{d^2u}{dx^2}\right)^2 - 18f_1\left(\frac{d^2u}{dx^2}\right)\left(\frac{d^3w_b}{dx^3}\right) - 24\left(\frac{df_3}{dz}\right)\left(\frac{d^2u}{dx^2}\right)\left(\frac{dw_b}{dx}\right) \\
&+ 18f_2\left(\frac{d^2u}{dx^2}\right)\left(\frac{d^3w_s}{dx^3}\right) - 48\left(\frac{df_3}{dz}\right)\left(\frac{d^2u}{dx^2}\right)\left(\frac{dw_s}{dx}\right) - 48\left(\frac{df_3}{dz}\right)\left(\frac{d^2u}{dx^2}\right)\left(\frac{dw_z}{dx}\right) \\
&+ 9{f_1}^2\left(\frac{d^3w_b}{dx^3}\right)^2 + 24f_1\left(\frac{df_3}{dz}\right)\left(\frac{d^3w_b}{dx^3}\right)\left(\frac{dw_b}{dx}\right) + 16\left(\frac{df_3}{dz}\right)^2\left(\frac{dw_b}{dx}\right)^2 \\
&- 18f_1f_2\left(\frac{d^3w_b}{dx^3}\right)\left(\frac{d^3w_s}{dx^3}\right) + 48f_1\left(\frac{df_3}{dz}\right)\left(\frac{d^3w_b}{dx^3}\right)\left(\frac{dw_s}{dx}\right) \\
&- 24f_2\left(\frac{df_3}{dz}\right)\left(\frac{dw_b}{dx}\right)\left(\frac{d^3w_s}{dx^3}\right) + 64\left(\frac{df_3}{dz}\right)^2\left(\frac{dw_b}{dx}\right)\left(\frac{dw_s}{dx}\right) \\
&+ 48f_1\left(\frac{df_3}{dz}\right)\left(\frac{d^3w_b}{dx^3}\right)\left(\frac{dw_z}{dx}\right) + 64\left(\frac{df_3}{dz}\right)^2\left(\frac{dw_b}{dx}\right)\left(\frac{dw_z}{dx}\right) + 9{f_2}^2\left(\frac{d^3w_s}{dx^3}\right)^2 \\
&- 48f_2\left(\frac{df_3}{dz}\right)\left(\frac{d^3w_s}{dx^3}\right)\left(\frac{dw_s}{dx}\right) + 64\left(\frac{df_3}{dz}\right)^2\left(\frac{dw_s}{dx}\right)^2 \\
&- 48f_2\left(\frac{df_3}{dz}\right)\left(\frac{d^3w_s}{dx^3}\right)\left(\frac{dw_z}{dx}\right) + 128\left(\frac{df_3}{dz}\right)^2\left(\frac{dw_s}{dx}\right)\left(\frac{dw_z}{dx}\right) \\
&+ 64\left(\frac{df_3}{dz}\right)^2\left(\frac{dw_z}{dx}\right)^2\Bigg] \qquad (A1l)
\end{aligned}
$$

$$
\begin{aligned}
3{\eta_{zxx}}^2 = \frac{3}{225}\Bigg[& 16(f_3)^2\left(\frac{d^2w_b}{dx^2}\right)^2 - 32\left(\frac{df_1}{dz}\right)(f_3)\left(\frac{d^2w_b}{dx^2}\right)^2 + 16\left(\frac{df_1}{dz}\right)^2\left(\frac{d^2w_b}{dx^2}\right)^2 \\
& + 64(f_3)^2\left(\frac{d^2w_b}{dx^2}\right)\left(\frac{d^2w_s}{dx^2}\right) - 64\left(\frac{df_1}{dz}\right)(f_3)\left(\frac{d^2w_b}{dx^2}\right)\left(\frac{d^2w_s}{dx^2}\right) \\
& + 32\left(\frac{df_2}{dz}\right)(f_3)\left(\frac{d^2w_b}{dx^2}\right)\left(\frac{d^2w_s}{dx^2}\right) - 32\left(\frac{df_1}{dz}\right)\left(\frac{df_2}{dz}\right)\left(\frac{d^2w_b}{dx^2}\right)\left(\frac{d^2w_s}{dx^2}\right) \\
& + 32(f_3)^2\left(\frac{d^2w_b}{dx^2}\right)\left(\frac{d^2w_z}{dx^2}\right) - 32\left(\frac{df_1}{dz}\right)(f_3)\left(\frac{d^2w_b}{dx^2}\right)\left(\frac{d^2w_z}{dx^2}\right) \\
& - 24(f_3)\left(\frac{d^2f_3}{dz^2}\right)\left(\frac{d^2w_b}{dx^2}\right)w_z + 24\left(\frac{df_1}{dz}\right)\left(\frac{d^2f_3}{dz^2}\right)\left(\frac{d^2w_b}{dx^2}\right)w_z + 64(f_3)^2\left(\frac{d^2w_s}{dx^2}\right)^2 \\
& + 64\left(\frac{df_2}{dz}\right)f_3\left(\frac{d^2w_s}{dx^2}\right)^2 + 16\left(\frac{df_2}{dz}\right)^2\left(\frac{d^2w_s}{dx^2}\right)^2 + 64(f_3)^2\left(\frac{d^2w_s}{dx^2}\right)\left(\frac{d^2w_z}{dx^2}\right) \\
& + 32\left(\frac{df_2}{dz}\right)(f_3)\left(\frac{d^2w_s}{dx^2}\right)\left(\frac{d^2w_z}{dx^2}\right) - 48(f_3)\left(\frac{d^2f_3}{dz^2}\right)\left(\frac{d^2w_s}{dx^2}\right)w_z \\
& - 24\left(\frac{df_2}{dz}\right)\left(\frac{d^2f_3}{dz^2}\right)\left(\frac{d^2w_s}{dx^2}\right)w_z \\
& + 16(f_3)^2\left(\frac{d^2w_z}{dx^2}\right)^2 + 9\left(\frac{d^2f_3}{dz^2}\right)^2{w_z}^2 - 24(f_3)\left(\frac{d^2f_3}{dz^2}\right)\left(\frac{d^2w_z}{dx^2}\right)w_z\Bigg] \qquad (A1m)
\end{aligned}
$$

$$3{\eta_{zyy}}^2 = \frac{3}{225}\Bigg[(f_3)^2\left(\frac{d^2w_b}{dx^2}\right)^2 - 2\left(\frac{df_1}{dz}\right) f_3\left(\frac{d^2w_b}{dx^2}\right)^2 + \left(\frac{df_1}{dz}\right)^2\left(\frac{d^2w_b}{dx^2}\right)^2$$

$$+ 4\,(f_3)^2\left(\frac{d^2w_b}{dx^2}\right)\left(\frac{d^2w_s}{dx^2}\right) - 4\left(\frac{df_1}{dz}\right) f_3\left(\frac{d^2w_b}{dx^2}\right)\left(\frac{d^2w_s}{dx^2}\right)$$

$$+ 2\left(\frac{df_2}{dz}\right) f_3\left(\frac{d^2w_b}{dx^2}\right)\left(\frac{d^2w_s}{dx^2}\right) - 2\left(\frac{df_1}{dz}\right)\left(\frac{df_2}{dz}\right)\left(\frac{d^2w_b}{dx^2}\right)\left(\frac{d^2w_s}{dx^2}\right)$$

$$+ 2\,(f_3)^2\left(\frac{d^2w_b}{dx^2}\right)\left(\frac{d^2w_z}{dx^2}\right) - 2\left(\frac{df_1}{dz}\right) f_3\left(\frac{d^2w_b}{dx^2}\right)\left(\frac{d^2w_z}{dx^2}\right)$$

$$+ 6f_3\left(\frac{d^2f_3}{dz^2}\right)\left(\frac{d^2w_b}{dx^2}\right)w_z - 6\left(\frac{df_1}{dz}\right)\left(\frac{d^2f_3}{dz^2}\right)\left(\frac{d^2w_b}{dx^2}\right)w_z + 4(f_3)^2\left(\frac{d^2w_s}{dx^2}\right)^2$$

$$+ 4\left(\frac{df_2}{dz}\right) f_3\left(\frac{d^2w_s}{dx^2}\right)^2 + \left(\frac{df_2}{dz}\right)^2\left(\frac{d^2w_s}{dx^2}\right)^2 + 4(f_3)^2\left(\frac{d^2w_s}{dx^2}\right)\left(\frac{d^2w_z}{dx^2}\right)$$

$$+ 2\left(\frac{df_2}{dz}\right) f_3\left(\frac{d^2w_s}{dx^2}\right)\left(\frac{d^2w_z}{dx^2}\right) + 12f_3\left(\frac{d^2f_3}{dz^2}\right)\left(\frac{d^2w_s}{dx^2}\right)w_z$$

$$+ 6\left(\frac{df_2}{dz}\right)\left(\frac{d^2f_3}{dz^2}\right)\left(\frac{d^2w_s}{dx^2}\right)w_z + (f_3)^2\left(\frac{d^2w_z}{dx^2}\right)^2$$

$$+ 9\left(\frac{d^2f_3}{dz^2}\right)^2 {w_z}^2 + 6f_3\left(\frac{d^2f_3}{dz^2}\right)\left(\frac{d^2w_z}{dx^2}\right)w_z\Bigg] \qquad (A1n)$$

2. Components of stiffness, mass and geometric stiffness matrices as well as force vector in Eq. (22) are presented in the form of:

$$K_{11}(i,j) = \int_0^l A\,\varphi_{i,x}\varphi_{j,x}dx + \int_0^l \left[A_\gamma + \frac{2}{5}A_\eta\right]\varphi_{i,xx}\varphi_{j,xx}dx \qquad (A2a)$$

$$K_{12}(i,j) = -\int_0^l B\,\varphi_{i,x}\varphi_{j,xx}dx - \int_0^l \left[B_\gamma + \frac{2}{5}B_\eta\right]\varphi_{i,xx}\varphi_{j,xxx}dx - \frac{1}{5}\int_0^l Y_\eta\,\varphi_{i,xx}\varphi_{j,x}dx \qquad (A2b)$$

$$K_{13}(i,j) = \int_0^l B_s\,\varphi_{i,x}\varphi_{j,xx}dx + \int_0^l \left[C_\gamma + \frac{2}{5}C_\eta\right]\varphi_{i,xx}\varphi_{j,xxx}dx - \frac{2}{5}\int_0^l Y_\eta\,\varphi_{i,xx}\varphi_{j,x}dx \qquad (A2c)$$

$$K_{14}(i,j) = \int_0^l X\,\varphi_{i,x}\varphi_{j}dx + \int_0^l \left[D_\gamma - \frac{2}{5}Y_\eta\right]\varphi_{i,xx}\varphi_{j,x}dx \qquad (A2d)$$

$$K_{22}(i,j) = \int_0^l \left[D + \frac{1}{8}A_\chi + H_\gamma + \frac{4}{15}Z_\eta + \frac{4}{15}S_\eta - \frac{8}{15}X_\eta\right]\varphi_{i,xx}\varphi_{j,xx}dx$$

$$+\int_0^l \left[A_s + \frac{1}{8}P_\chi + \frac{4}{15}R_\eta\right]\varphi_{i,x}\varphi_{j,x}dx + \int_0^l \left[F_\gamma + \frac{2}{5}D_\eta\right]\varphi_{i,xxx}\varphi_{j,xxx}dx + \int_0^l \frac{2}{5}F_{s\eta}\,\varphi_{i,xxx}\varphi_{j,x}dx \qquad (A2e)$$

$$K_{23}(i,j) = \int_0^l \left[-D_s + \frac{1}{8}B_\chi - Y_\gamma - \frac{4}{15}B_{s\eta} + \frac{4}{15}C_{s\eta} + \frac{8}{15}S_\eta - \frac{8}{15}X_\eta\right]\varphi_{i,xx}\varphi_{j,xx}dx$$

$$+\int_0^l \left[2A_s - \frac{1}{8}R_\chi + \frac{8}{15}R_\eta\right]\varphi_{i,x}\varphi_{j,x}dx - \int_0^l \left[X_\gamma + \frac{2}{5}H_\eta\right]\varphi_{i,xxx}\varphi_{j,xxx}dx + \int_0^l \frac{2}{5}F_{s\eta}\,\varphi_{i,xxx}\varphi_{j,x}dx$$

$$-\int_0^l \frac{1}{5}H_{s\eta}\,\varphi_{i,x}\varphi_{j,xxx}dx \qquad (A2f)$$

$$K_{24}(i,j) = \int_0^l \left[-Y - P_\gamma + \frac{1}{5}Y_{s\eta} - \frac{1}{5}D_{s\eta}\right]\varphi_{i,xx}\varphi_j dx + \int_0^l \left[A_s + \frac{1}{8}S_\chi + \frac{8}{15}R_\eta\right]\varphi_{i,x}\varphi_{j,x}dx$$

$$+\int_0^l \left[\frac{1}{8}D_\chi - \frac{4}{15}X_\eta + \frac{4}{15}S_\eta\right]\varphi_{i,xx}\varphi_{i,xx}dx + \int_0^l \left[-Z_\gamma + \frac{2}{5}F_{s\eta}\right]\varphi_{i,xxx}\varphi_{j,x}dx \qquad (A2g)$$

$$K_{33}(i,j) = \int_0^l \left[H + \frac{1}{8}C_\chi + S_\gamma + \frac{4}{15}P_\eta + \frac{16}{15}C_{s\eta} + \frac{16}{15}S_\eta\right]\varphi_{i,xx}\varphi_{j,xx}dx - \frac{4}{5}\int_0^l H_{s\eta}\,\varphi_{i,xxx}\varphi_{j,x}dx$$

$$+ \int_0^l \left[R_\gamma + \frac{2}{5}F_\eta\right]\varphi_{i,xxx}\varphi_{j,xxx}dx + \int_0^l \left[4A_s + \frac{1}{8}X_\chi + \frac{16}{15}R_\eta\right]\varphi_{i,x}\varphi_{j,x}dx \qquad (A2h)$$

$$K_{34}(i,j) = \int_0^l \left[Y_s + B_{s\gamma} - \frac{1}{5}R_{s\eta} - \frac{2}{5}D_{s\eta}\right]\varphi_{i,xx}\varphi_j dx + \int_0^l \left[2A_s - \frac{1}{8}Z_\chi + \frac{16}{15}R_\eta\right]\varphi_{i,x}\varphi_{j,x}dx$$

$$+ \int_0^l \left[\frac{1}{8}H_\chi + \frac{4}{15}C_{s\eta} + \frac{8}{15}S_\eta\right]\varphi_{i,xx}\varphi_{j,xx}dx + \int_0^l \left[A_{s\gamma} - \frac{2}{5}H_{s\eta}\right]\varphi_{i,xxx}\varphi_{j,x}dx \qquad (A2i)$$

$$K_{44}(i,j) = \int_0^l \left[Z + D_{s\gamma} + \frac{2}{5}A_{s\eta}\right]\varphi_i\varphi_j dx + \int_0^l \left[A_s + \frac{1}{8}Y_\chi + C_{s\gamma} + \frac{16}{15}R_\eta\right]\varphi_{i,x}\varphi_{j,x}dx$$

$$+ \int_0^l \left[\frac{1}{8}F_\chi + \frac{4}{15}S_\eta\right]\varphi_{i,xx}\varphi_{j,xx}dx - \frac{2}{5}\int_0^l D_{s\eta}\,\varphi_{i,xx}\varphi_j dx \qquad (A2j)$$

$$M_{11}(i,j) = \int_0^l I_0\,\varphi_i\varphi_j dx \qquad (A2k)$$

$$M_{12}(i,j) = -\int_0^l I_1\,\varphi_i\varphi_{j,x}dx \qquad (A2l)$$

$$M_{13}(i,j) = \int_0^l J_1\,\varphi_i\varphi_{j,x}dx \qquad (A2m)$$

$$M_{22}(i,j) = \int_0^l I_0\,\varphi_i\varphi_j dx + \int_0^l I_2\,\varphi_{i,x}\varphi_{j,x}dx \qquad (A2n)$$

$$M_{23}(i,j) = \int_0^l I_0\,\varphi_i\varphi_j dx - \int_0^l J_3\,\varphi_{i,x}\varphi_{j,x}dx \qquad (A2o)$$

$$M_{24}(i,j) = \int_0^l J_2\,\varphi_i\varphi_j dx \qquad (A2p)$$

$$M_{33}(i,j) = \int_0^l I_0\,\varphi_i\varphi_j dx + \int_0^l K_1\,\varphi_{i,x}\varphi_{j,x}dx \qquad (A2q)$$

$$M_{34}(i,j) = \int_0^l J_2\, \varphi_i \varphi_j dx \quad (A2r)$$

$$M_{44}(i,j) = \int_0^l K_2\, \varphi_i \varphi_j dx \quad (A2s)$$

$$G_{22}(i,j) = -N_0 \int_0^l \varphi_{i,x} \varphi_{j,x}\, dx \quad (A2t)$$

$$G_{23}(i,j) = -N_0 \int_0^l \varphi_{i,x} \varphi_{j,x}\, dx \quad (A2u)$$

$$G_{33}(i,j) = -N_0 \int_0^l \varphi_{i,x} \varphi_{j,x}\, dx \quad (A2v)$$

$$F_2(i) = -\int_0^l q(x) \varphi_i\, dx \quad (A2w)$$

$$F_3(i) = -\int_0^l q(x) \varphi_i\, dx \quad (A2x)$$

Here, the stiffness coefficients can be defined by:

$$(A, B, B_s, D, D_s, H, Z) = \int_{-h/2}^{+h/2} Q_{11} \left(1, f_1, f_2, {f_1}^2, f_1 f_2, {f_2}^2, {f_3'}^2\right) dz \quad (A3a)$$

$$A_s = \int_{-h/2}^{+h/2} Q_{44} {f_3}^2 dz \quad (A3b)$$

$$(X, Y, Y_s) = \int_{-h/2}^{+h/2} Q_{13} f_3' (1, f_1, f_2) dz \quad (A3c)$$

$$\begin{aligned}(A_\chi, B_\chi, C_\chi, D_\chi, F_\chi, H_\chi, X_\chi, Y_\chi, Z_\chi, P_\chi, R_\chi, S_\chi) \\ = \int_{-h/2}^{+h/2} \frac{E {\ell_2}^2}{1+\nu} \Big[&(1+f_1')^2, (1+f_1')(1-f_2'), (1-f_2')^2, (1+f_1')f_3, {f_3}^2, (1 \\ &- f_2')f_3, {f_2''}^2, {f_3'}^2, f_2'' f_3', {f_1''}^2, f_1'' f_2'', f_1'' f_3'\Big] dz\end{aligned} \quad (A3d)$$

$$\begin{aligned}(A_\gamma, B_\gamma, C_\gamma, D_\gamma, F_\gamma, H_\gamma, X_\gamma, Y_\gamma, Z_\gamma, P_\gamma, R_\gamma, S_\gamma, A_{s\gamma}, B_{s\gamma}, C_{s\gamma}, D_{s\gamma}) \\ = \int_{-h/2}^{+h/2} \frac{E {\ell_0}^2}{1+\nu} \Big[1, f_1, f_2, f_3', {f_1}^2, {f_1'}^2, f_1 f_2, f_1' f_2', f_1 f_3', f_1' f_3'', {f_2}^2, {f_2'}^2, f_2 f_3', f_2' f_3'', {f_3'}^2, {f_3''}^2\Big] dz\end{aligned} \quad (A3e)$$

$$(A_\eta, B_\eta, C_\eta, D_\eta, F_\eta, H_\eta, X_\eta, Y_\eta, Z_\eta, P_\eta, R_\eta, S_\eta, A_{s\eta}, B_{s\eta}, C_{s\eta}, D_{s\eta}, F_{s\eta}, H_{s\eta}, Y_{s\eta}, R_{s\eta})$$

$$= \int_{-\frac{h}{2}}^{+\frac{h}{2}} \frac{E{\ell_1}^2}{1+\nu}\Big[1, f_1, f_2, {f_1}^2, {f_2}^2, f_1 f_2, f_1' f_3, f_3', {f_1'}^2, {f_2'}^2, {f_3'}^2, {f_3}^2, {f_3''}^2, f_1' f_2', f_2' f_3, f_3 f_3'',$$
$$f_1 f_3', f_2 f_3', f_1' f_3'', f_2' f_3''\Big] dz \qquad (A3f)$$

3. The equations of motion are presented in the form of:

$$\frac{\partial}{\partial x}\left(A\frac{\partial u}{\partial x}\right) - \frac{\partial^2}{\partial x^2}\left[\left(A_\gamma + \frac{2}{5}A_\eta\right)\frac{\partial^2 u}{\partial x^2}\right] - \frac{\partial}{\partial x}\left(B\frac{\partial^2 w_b}{\partial x^2}\right) + \frac{\partial^2}{\partial x^2}\left[\left(B_\gamma + \frac{2}{5}B_\eta\right)\frac{\partial^3 w_b}{\partial x^3}\right]$$
$$+ \frac{1}{5}\frac{\partial^2}{\partial x^2}\left(Y_\eta \frac{\partial w_b}{\partial x}\right) + \frac{\partial}{\partial x}\left(B_s\frac{\partial^2 w_s}{\partial x^2}\right) - \frac{\partial^2}{\partial x^2}\left[\left(C_\gamma + \frac{2}{5}C_\eta\right)\frac{\partial^3 w_s}{\partial x^3}\right] + \frac{2}{5}\frac{\partial^2}{\partial x^2}\left(Y_\eta\frac{\partial w_s}{\partial x}\right)$$
$$+ \frac{\partial}{\partial x}(X w_z) - \frac{\partial^2}{\partial x^2}\left[\left(D_\gamma - \frac{2}{5}Y_\eta\right)\frac{\partial w_z}{\partial x}\right]$$
$$= I_0 \ddot{u} - I_1\frac{\partial \ddot{w}_b}{\partial x} - J_1\frac{\partial \ddot{w}_s}{\partial x} \qquad (A4a)$$

$$\frac{\partial^2}{\partial x^2}\left(B\frac{\partial u}{\partial x}\right) + \frac{\partial^3}{\partial x^3}\left[\left(B_\gamma + \frac{2}{5}B_\eta\right)\frac{\partial^2 u}{\partial x^2}\right] + \frac{1}{5}\frac{\partial}{\partial x}\left(Y_\eta\frac{\partial^2 u}{\partial x^2}\right)$$
$$- \frac{\partial^2}{\partial x^2}\left[\left(D + \frac{1}{8}A_\chi + H_\gamma + \frac{4}{15}Z_\eta + \frac{4}{15}S_\eta - \frac{8}{15}X_\eta\right)\frac{\partial^2 w_b}{\partial x^2}\right]$$
$$- \frac{\partial}{\partial x}\left[\left(A_s + \frac{1}{8}P_\chi + \frac{4}{15}R_\eta\right)\frac{\partial w_b}{\partial x}\right] - \frac{\partial^3}{\partial x^3}\left[\left(F_\gamma + \frac{2}{5}D_\eta\right)\frac{\partial^3 w_b}{\partial x^3}\right] - \frac{2}{5}\frac{\partial}{\partial x}\left(F_{s\eta}\frac{\partial^3 w_b}{\partial x^3}\right)$$
$$- \frac{\partial^2}{\partial x^2}\left[\left(-D_s + \frac{1}{8}B_\chi - Y_\gamma - \frac{4}{15}B_{s\eta} + \frac{4}{15}C_{s\eta} + \frac{8}{15}S_\eta - \frac{8}{15}X_\eta\right)\frac{\partial^2 w_s}{\partial x^2}\right]$$
$$+ \frac{\partial}{\partial x}\left[\left(2A_s - \frac{1}{8}R_\chi + \frac{8}{15}R_\eta\right)\frac{\partial w_s}{\partial x}\right] + \frac{\partial^3}{\partial x^3}\left[\left(X_\gamma + \frac{2}{5}H_\eta\right)\frac{\partial^3 w_s}{\partial x^3}\right] - \frac{2}{5}\frac{\partial^3}{\partial x^3}\left(F_{s\eta}\frac{\partial w_s}{\partial x}\right)$$
$$- \frac{1}{5}\frac{\partial}{\partial x}\left(H_{s\eta}\frac{\partial^3 w_s}{\partial x^3}\right) - \frac{\partial^2}{\partial x^2}\left[\left(-Y - P_\gamma + \frac{1}{5}Y_{s\eta} - \frac{1}{5}D_{s\eta}\right)w_z\right]$$
$$+ \frac{\partial}{\partial x}\left[\left(A_s + \frac{1}{8}S_\chi + \frac{8}{15}R_\eta\right)\frac{\partial w_z}{\partial x}\right] - \frac{\partial^2}{\partial x^2}\left[\left(\frac{1}{8}D_\chi - \frac{4}{15}X_\eta + \frac{4}{15}S_\eta\right)\frac{\partial^2 w_z}{\partial x^2}\right]$$
$$- \frac{\partial^3}{\partial x^3}\left[\left(-Z_\gamma + \frac{2}{5}F_{s\eta}\right)\frac{\partial w_z}{\partial x}\right] + N_0\frac{\partial^2 w_b}{\partial x^2} + N_0\frac{\partial^2 w_s}{\partial x^2} + N_0\frac{\partial^2 w_z}{\partial x^2} + q$$
$$= I_0\frac{\partial \ddot{w}_b}{\partial x} + I_2\frac{\partial^2 \ddot{w}_b}{\partial x^2} + I_0\frac{\partial \ddot{w}_s}{\partial x} - J_3\frac{\partial^2 \ddot{w}_s}{\partial x^2} + J_2\frac{\partial \ddot{w}_z}{\partial x} - I_1\frac{\partial \ddot{u}}{\partial x} \qquad (A4b)$$

$$
\begin{aligned}
&-\frac{\partial^2}{\partial x^2}\left(B_s\frac{\partial u}{\partial x}\right)-\frac{\partial^3}{\partial x^3}\left[\left(C_\gamma+\frac{2}{5}C_\eta\right)\frac{\partial^2 u}{\partial x^2}\right]+\frac{1}{5}\frac{\partial}{\partial x}\left(Y_\eta\frac{\partial^2 u}{\partial x^2}\right)\\
&\quad-\frac{\partial^2}{\partial x^2}\left[\left(D_s+\frac{1}{8}B_\chi-Y_\gamma-\frac{4}{15}B_{s\eta}+\frac{4}{15}C_{s\eta}+\frac{8}{15}S_\eta-\frac{8}{15}X_\eta\right)\frac{\partial^2 w_b}{\partial x^2}\right]\\
&\quad-\frac{\partial}{\partial x}\left[\left(2A_s-\frac{1}{8}R_\chi+\frac{8}{15}R_\eta\right)\frac{\partial w_b}{\partial x}\right]+\frac{\partial^3}{\partial x^3}\left[\left(X_\gamma+\frac{2}{5}H_\eta\right)\frac{\partial^3 w_b}{\partial x^3}\right]-\frac{2}{5}\frac{\partial}{\partial x}\left(F_{s\eta}\frac{\partial^3 w_b}{\partial x^3}\right)\\
&\quad+\frac{2}{5}\frac{\partial^3}{\partial x^3}\left(H_{s\eta}\frac{\partial w_b}{\partial x}\right)-\frac{\partial^2}{\partial x^2}\left[\left(H+\frac{1}{8}C_\chi+S_\gamma+\frac{4}{15}P_\eta+\frac{16}{15}C_{s\eta}+\frac{16}{15}S_\eta\right)\frac{\partial^2 w_s}{\partial x^2}\right]\\
&\quad-\frac{\partial}{\partial x}\left[\left(4A_s+\frac{1}{8}X_\chi+\frac{16}{15}R_\eta\right)\frac{\partial w_s}{\partial x}\right]-\frac{\partial^3}{\partial x^3}\left[\left(R_\gamma+\frac{2}{5}F_\eta\right)\frac{\partial^3 w_s}{\partial x^3}\right]+\frac{4}{5}\frac{\partial}{\partial x}\left(H_{s\eta}\frac{\partial^3 w_s}{\partial x^3}\right)\\
&\quad-\frac{\partial^2}{\partial x^2}\left[\left(Y_s+B_{s\gamma}-\frac{1}{5}R_{s\eta}-\frac{2}{5}D_{s\eta}\right)w_z\right]+\frac{\partial}{\partial x}\left[\left(2A_s-\frac{1}{8}Z_\chi+\frac{16}{15}R_\eta\right)\frac{\partial w_z}{\partial x}\right]\\
&\quad-\frac{\partial^2}{\partial x^2}\left[\left(\frac{1}{8}H_\chi+\frac{4}{15}C_{s\eta}+\frac{8}{15}S_\eta\right)\frac{\partial^2 w_z}{\partial x^2}\right]-\frac{\partial^3}{\partial x^3}\left[\left(A_{s\gamma}-\frac{2}{5}H_{s\eta}\right)\frac{\partial w_z}{\partial x}\right]+N_0\frac{\partial^2 w_b}{\partial x^2}\\
&\quad+N_0\frac{\partial^2 w_s}{\partial x^2}+N_0\frac{\partial^2 w_z}{\partial x^2}+q\\
&\quad=I_0\,\frac{\partial \ddot{w}_s}{\partial x}+K_1\,\frac{\partial^2 \ddot{w}_s}{\partial x^2}+J_2\,\frac{\partial \ddot{w}_z}{\partial x}++J_1\,\frac{\partial \ddot{u}}{\partial x}\;I_0\,\frac{\partial \ddot{w}_b}{\partial x}-J_3\,\frac{\partial^2 \ddot{w}_b}{\partial x^2} \qquad (A4c)
\end{aligned}
$$

$$
\begin{aligned}
&X\frac{\partial u}{\partial x}-\frac{\partial}{\partial x}\left[\left(D_\gamma-\frac{2}{5}Y_\eta\right)\frac{\partial^2 u}{\partial x^2}\right]+\left(-Y-P_\gamma+\frac{1}{5}Y_{s\eta}-\frac{1}{5}D_{s\eta}\right)\frac{\partial^2 w_b}{\partial x^2}\\
&\quad-\frac{\partial}{\partial x}\left[\left(A_s+\frac{1}{8}S_\chi+\frac{8}{15}R_\eta\right)\frac{\partial w_b}{\partial x}\right]-\frac{\partial^2}{\partial x^2}\left[\left(\frac{1}{8}D_\chi-\frac{4}{15}X_\eta+\frac{4}{15}S_\eta\right)\frac{\partial^2 w_b}{\partial x^2}\right]\\
&\quad-\frac{\partial}{\partial x}\left[\left(-Z_\gamma+\frac{2}{5}F_{s\eta}\right)\frac{\partial^3 w_b}{\partial x^3}\right]+\left(Y_s+B_{s\gamma}-\frac{1}{5}R_{s\eta}-\frac{2}{5}D_{s\eta}\right)\frac{\partial^2 w_s}{\partial x^2}\\
&\quad-\frac{\partial}{\partial x}\left[\left(2A_s-\frac{1}{8}Z_\chi+\frac{16}{15}R_\eta\right)\frac{\partial w_s}{\partial x}\right]-\frac{\partial^2}{\partial x^2}\left[\left(\frac{1}{8}H_\chi+\frac{4}{15}C_{s\eta}+\frac{8}{15}S_\eta\right)\frac{\partial^2 w_s}{\partial x^2}\right]\\
&\quad-\frac{\partial}{\partial x}\left[\left(A_{s\gamma}-\frac{2}{5}H_{s\eta}\right)\frac{\partial^3 w_s}{\partial x^3}\right]+\left(Z+D_{s\gamma}+\frac{2}{5}A_{s\eta}\right)w_z\\
&\quad-\frac{\partial}{\partial x}\left[\left(A_s+\frac{1}{8}Y_\chi+C_{s\gamma}+\frac{16}{15}R_\eta\right)\frac{\partial w_z}{\partial x}\right]-\frac{\partial^2}{\partial x^2}\left[\left(\frac{1}{8}F_\chi+\frac{4}{15}S_\eta\right)\frac{\partial^2 w_z}{\partial x^2}\right]-\frac{2}{5}D_{s\eta}\frac{\partial^2 w_z}{\partial x^2}\\
&\quad+N_0\frac{\partial^2 w_b}{\partial x^2}+N_0\frac{\partial^2 w_s}{\partial x^2}+N_0\frac{\partial^2 w_z}{\partial x^2}=K_2\,\frac{\partial \ddot{w}_z}{\partial x}+J_2\,\frac{\partial \ddot{w}_b}{\partial x}+J_2\,\frac{\partial \ddot{w}_s}{\partial x} \qquad (A4d)
\end{aligned}
$$

Table 1. Kinematic boundary conditions for 2NBE used for the numerical computations.

BC	x=0	x=L
SS	$u=0, w_b=0, w_s=0, w_z=0$	$w_b=0, w_s=0, w_z=0$
CC	$u=0, w_b=0, w_s=0, w_z=0,$ $w_b{}'=0, w_s{}'=0, w_z{}'=0$	$u=0, w_b=0, w_s=0, w_z=0,$ $w_b{}'=0, w_s{}'=0, w_z{}'=0$
CF	$u=0, w_b=0, w_s=0, w_z=0,$ $w_b{}'=0, w_s{}'=0$	

Table 2. Convergence studies on the DFFs of S-S and C-C 2D FG microbeams for various p_x $(L/h = 10, h/\ell_c = 1, p_z = 1)$.

BC	Number of elements	2NBE			3NBE		
		$p_x = 1$	2	5	$p_x = 1$	2	5
MCST							
SS	30 elements	3.3683	2.7875	2.3085	3.3683	2.7875	2.3085
	40 elements	3.3683	2.7875	2.3085	3.3683	2.7875	2.3085
	50 elements	3.3683	2.7875	2.3085	3.3683	2.7875	2.3085
	60 elements	3.3683	2.7875	2.3085	3.3683	2.7875	2.3085
	70 elements	3.3683	2.7875	2.3085	3.3683	2.7875	2.3085
	80 elements	3.3683	2.7875	2.3085	3.3683	2.7875	2.3085
	Chen et al. [54] (TBT, MCST)	3.3901	2.7944	2.3019	3.3901	2.7944	2.3019
CC	30 elements	7.4434	6.6671	5.9298	7.4430	6.6668	5.9296
	40 elements	7.4431	6.6669	5.9297	7.4430	6.6668	5.9296
	50 elements	7.4431	6.6669	5.9296	7.4430	6.6668	5.9296
	60 elements	7.4430	6.6668	5.9296	7.4430	6.6668	5.9296
	70 elements	7.4430	6.6668	5.9296	7.4430	6.6668	5.9296
	80 elements	7.4430	6.6668	5.9296	7.4430	6.6668	5.9296
	Chen et al. [54] (TBT, MCST)	7.4437	6.6480	5.9074	7.4437	6.6480	5.9074
MSGT							
SS	30 elements	5.0100	4.0975	3.3602	5.0099	4.0974	3.3601
	40 elements	5.0089	4.0965	3.3593	5.0089	4.0964	3.3593
	50 elements	5.0084	4.0960	3.3588	5.0083	4.0959	3.3588
	60 elements	5.0080	4.0957	3.3586	5.0080	4.0956	3.3586
	70 elements	5.0078	4.0955	3.3584	5.0078	4.0955	3.3584
	80 elements	5.0077	4.0953	3.3583	5.0077	4.0953	3.3583
CC	30 elements	11.2228	9.9408	8.7249	11.2167	9.9357	8.7208
	40 elements	11.2082	9.9288	8.7146	11.2044	9.9257	8.7121
	50 elements	11.1998	9.9221	8.7088	11.1973	9.9200	8.7071
	60 elements	11.1945	9.9178	8.7051	11.1927	9.9163	8.7040
	70 elements	11.1908	9.9148	8.7027	11.1895	9.9138	8.7018
	80 elements	11.1882	9.9128	8.7010	11.1872	9.9120	8.7003

Table 3. Verification studies on the DFFs of S-S and C-C 2D FG microbeams for various $p_x, p_z, h/\ell_c$ $(L/h = 10)$

h/ℓ_c	p_z	Chen et al. [54] (TBT, MCST)				Present (Q3D TBT, MCST)				Present (Q3D TBT, MSGT)			
		$p_x = 1$	2	5	10	$p_x = 1$	2	5	10	$p_x = 1$	2	5	10
S-S													
1	1	3.3901	2.7944	2.3019	2.1676	3.3683	2.7875	2.3085	2.1780	5.0078	4.0955	3.3584	3.1583
	2	3.0481	2.6212	2.2575	2.1560	3.0356	2.6193	2.2653	2.1668	4.4962	3.8354	3.2904	3.1399
	5	2.6818	2.4291	2.2061	2.1427	2.6809	2.4333	2.2155	2.1537	3.9208	3.5351	3.2095	3.1179
	10	2.4817	2.3199	2.1759	2.1348	2.4863	2.3271	2.1861	2.1460	3.6045	3.3660	3.1627	3.1050
2	1	2.2273	1.8960	1.6030	1.5193	2.2311	1.9032	1.6123	1.5290	2.9285	2.4430	2.0347	1.9211
	2	2.0321	1.7965	1.5774	1.5125	2.0402	1.8055	1.5868	1.5222	2.6556	2.3035	1.9982	1.9112
	5	1.8486	1.6969	1.5494	1.5048	1.8599	1.7071	1.5590	1.5144	2.3675	2.1506	1.9560	1.8995
	10	1.7428	1.6349	1.5309	1.4997	1.7542	1.6452	1.5405	1.5093	2.2034	2.0596	1.9300	1.8922
8	1	1.7030	1.5050	1.3093	1.2494	1.7231	1.5215	1.3208	1.2592	1.7946	1.5735	1.3592	1.2945
	2	1.5818	1.4423	1.2928	1.2448	1.6030	1.4585	1.3039	1.2544	1.6645	1.5056	1.3411	1.2894
	5	1.4933	1.3897	1.2761	1.2396	1.5124	1.4041	1.2865	1.2491	1.5601	1.4445	1.3222	1.2836
	10	1.4340	1.3503	1.2629	1.2357	1.4502	1.3631	1.2729	1.2451	1.4909	1.4002	1.3078	1.2794
C-C													
1	1	7.4437	6.6480	5.9074	5.5252	7.4430	6.6668	5.9296	5.5479	11.1908	9.9148	8.7027	8.0779
	2	6.7315	6.1562	5.6156	5.3368	6.7421	6.1795	5.6416	5.3634	10.1604	9.2123	8.3061	7.8367
	5	5.9483	5.6054	5.2787	5.1106	5.9712	5.6348	5.3102	5.1431	8.9433	8.3713	7.8170	7.5272
	10	5.5130	5.2931	5.0819	4.9733	5.5410	5.3255	5.1166	5.0093	8.2266	7.8648	7.5105	7.3240
2	1	4.8377	4.3960	3.9768	3.7606	4.8780	4.4424	4.0161	3.7958	6.4737	5.8077	5.1664	4.8338
	2	4.4245	4.1080	3.8027	3.6464	4.4678	4.1532	3.8427	3.6836	5.9092	5.4171	4.9406	4.6937
	5	4.0218	3.8213	3.6240	3.5246	4.0649	3.8638	3.6645	3.5641	5.2872	4.9801	4.6802	4.5258
	10	3.7966	3.6569	3.5188	3.4499	3.8377	3.6977	3.5592	3.4900	4.9224	4.7188	4.5192	4.4167
8	1	3.6383	3.3754	3.1174	2.9856	3.7008	3.4361	3.1649	3.0262	3.8700	3.5775	3.2810	3.1285
	2	3.3750	3.1896	3.0025	2.9087	3.4364	3.2460	3.0489	2.9500	3.5856	3.3741	3.1579	3.0485
	5	3.1674	3.0389	2.9068	2.8427	3.2216	3.0880	2.9504	2.8833	3.3422	3.1965	3.0479	2.9748
	10	3.0482	2.9495	2.8489	2.8006	3.0971	2.9947	2.8904	2.8400	3.2011	3.0917	2.9809	2.9270

Table 4. Verification studies on the DCBLs of S-S and C-C 2D FG microbeams for various $p_x, p_z, h/\ell_c$ $(L/h = 10)$

h/ℓ_c	p_z	Chen et al. [54] (TBT, MCST)				Present (Q3D TBT, MCST)				Present (Q3D TBT, MSGT)			
		$p_x = 1$	2	5	10	$p_x = 1$	2	5	10	$p_x = 1$	2	5	10
S-S													
1	1	12.6586	8.4676	5.7910	5.1597	12.3070	8.2709	5.6975	5.0899	27.2141	17.8611	12.0902	10.7402
	2	10.2423	7.4970	5.5834	5.1068	9.9838	7.3374	5.4969	5.0386	21.9309	15.7525	11.6321	10.6191
	5	7.9267	6.4698	5.3431	5.0450	7.7626	6.3522	5.2656	4.9788	16.6486	13.4449	11.0889	10.4737
	10	6.7824	5.9112	5.2014	5.0083	6.6603	5.8147	5.1292	4.9432	14.0475	12.2078	10.7754	10.3880
2	1	5.5042	3.9252	2.8135	2.5355	5.4377	3.8800	2.7828	2.5086	9.3438	6.3789	4.4387	3.9704
	2	4.5770	3.5380	2.7286	2.5135	4.5314	3.5001	2.6990	2.4866	7.6683	5.6934	4.2878	3.9302
	5	3.7744	3.1614	2.6355	2.4883	3.7422	3.1292	2.6069	2.4614	6.0699	4.9740	4.1143	3.8829
	10	3.3466	2.9360	2.5742	2.4716	3.3161	2.9055	2.5463	2.4449	5.2434	4.5653	4.0076	3.8534
8	1	3.2431	2.4911	1.8803	1.7150	3.2673	2.4959	1.8703	1.7017	3.5415	2.6676	1.9814	1.7993
	2	2.7877	2.2908	1.8347	1.7025	2.8109	2.2933	1.8237	1.6889	3.0299	2.4431	1.9301	1.7852
	5	2.4677	2.1233	1.7879	1.6884	2.4787	2.1192	1.7753	1.6744	2.6379	2.2436	1.8760	1.7692
	10	2.2672	2.0032	1.7516	1.6779	2.2673	1.9946	1.7383	1.6638	2.3976	2.1059	1.8359	1.7577
C-C													
1	1	47.5068	35.4722	26.8071	23.5943	46.7543	35.0572	26.5157	23.3602	104.9270	76.6292	56.5523	49.3437
	2	38.9911	31.0395	24.9399	22.5843	38.3969	30.6810	24.6872	22.3773	86.5405	67.3321	52.8604	47.4324
	5	30.5226	26.2837	22.7684	21.3441	30.1181	26.0095	22.5707	21.1796	67.1035	56.7716	48.3204	44.9586
	10	26.2202	23.6877	21.4924	20.5781	25.9172	23.4671	21.3305	20.4424	56.8050	50.7335	45.5065	43.3478
2	1	20.3891	15.8694	12.4361	11.1423	20.4347	15.9432	12.4558	11.1518	35.5787	26.7738	20.2809	17.9049
	2	17.0807	14.0962	11.6680	10.7217	17.1173	14.1454	11.6891	10.7373	29.6233	23.6683	19.0113	17.2387
	5	14.0982	12.3750	10.8684	10.2623	14.1196	12.4021	10.8917	10.2858	23.6858	20.3453	17.5424	16.4265
	10	12.5366	11.4071	10.3882	9.9706	12.5491	11.4272	10.4127	9.9974	20.5106	18.4418	16.6358	15.8969
8	1	11.7956	9.6547	7.8907	7.2173	12.0541	9.8570	7.9959	7.2941	13.1297	10.6240	8.5452	7.7629
	2	10.1387	8.7321	7.4793	6.9893	10.3534	8.8943	7.5766	7.0658	11.2306	9.5607	8.0857	7.5142
	5	8.8916	7.9858	7.1307	6.7894	9.0433	8.1024	7.2154	6.8618	9.7007	8.6454	7.6686	7.2793
	10	8.1984	7.5365	6.9058	6.6498	8.3140	7.6309	6.9811	6.7169	8.8563	8.1059	7.4019	7.1158

Table 5. DMDs of S-S and C-C 2D FG microbeams for various $p_x, p_z, h/\ell_c$ $(L/h = 10)$

h/ℓ_c	p_z	Present (Q3D TBT, MCST)				Present (Q3D TBT, MSGT)			
		$p_x = 1$	2	5	10	$p_x = 1$	2	5	10
S-S									
1	1	19.8611	29.5606	44.2904	49.9169	8.9577	13.6625	20.9124	23.7305
	2	24.8062	33.8181	46.0600	50.4188	11.2777	15.7444	21.8199	23.9977
	5	32.3136	39.5786	48.1949	51.0048	15.0824	18.7332	22.9538	24.3216
	10	37.8754	43.4660	49.5017	51.3522	17.9995	20.7605	23.6373	24.5141
2	1	45.3960	63.5380	90.7793	101.2698	26.2691	38.4742	56.9728	64.1308
	2	55.0335	71.2397	93.8349	102.1520	32.4039	43.7003	59.1658	64.7806
	5	67.1813	80.3952	97.3207	103.1608	41.4104	50.6271	61.8047	65.5467
	10	76.0870	86.9367	99.6925	103.8238	48.1919	55.4485	63.4901	66.0230
8	1	76.2882	99.5621	135.2041	149.2690	70.2894	93.0615	127.6585	141.2476
	2	89.2708	109.2100	138.9065	150.3801	82.7642	102.4734	131.3057	142.3416
	5	101.6201	118.7804	142.8702	151.6385	95.4939	112.2294	135.2736	143.5860
	10	111.3070	126.5758	145.9944	152.5610	105.3007	119.9502	138.3116	144.4795
C-C									
1	1	4.0988	5.1908	6.7770	7.8282	1.8068	2.3378	3.1440	3.6963
	2	5.1020	6.1520	7.5473	8.4038	2.2398	2.7597	3.4805	3.9394
	5	6.6494	7.5285	8.5754	9.1630	2.9607	3.4079	3.9595	4.2817
	10	7.8054	8.4944	9.2595	9.6676	3.5416	3.8961	4.3023	4.5274
2	1	9.6214	11.7896	14.8442	16.7645	5.4292	6.8549	8.9454	10.3302
	2	11.6871	13.6920	16.3124	17.8428	6.6499	8.0132	9.8526	10.9853
	5	14.3798	16.0347	18.0220	19.0917	8.4841	9.6388	11.0469	11.8412
	10	16.2790	17.6208	19.1415	19.9240	9.8920	10.8203	11.8773	12.4436
8	1	16.8526	19.8628	24.0091	26.4402	15.3848	18.2950	22.3210	24.7274
	2	19.8619	22.5195	25.9771	27.8638	18.2218	20.8196	24.2010	26.0822
	5	22.9362	25.1352	27.8225	29.1923	21.2983	23.4464	26.0625	27.4156
	10	25.0049	26.8671	29.0335	30.1028	23.3983	25.2019	27.2899	28.3313

Table 6. DFFs/DCBLs/DMDs of C-F 2D FG microbeams for various $p_x, p_z, h/\ell_c$ $(L/h = 10)$

h/ℓ_c	p_z	DFFs				DCBLs				DMDs			
		$p_x = 1$	2	5	10	$p_x = 1$	2	5	10	$p_x = 1$	2	5	10
MCST													
1	1	2.0973	1.8482	1.7535	1.7513	2.1498	1.5831	1.3013	1.2471	129.0134	162.2757	174.4759	174.8922
	2	2.0173	1.8311	1.7592	1.7570	1.8935	1.4942	1.2842	1.2431	139.4130	165.6164	174.5993	174.8941
	5	1.9257	1.8102	1.7647	1.7627	1.6257	1.3941	1.2643	1.2385	152.1698	169.3275	174.7293	174.8935
	10	1.8711	1.7963	1.7668	1.7653	1.4812	1.3362	1.2524	1.2358	160.0336	171.4220	174.7960	174.8963
2	1	1.4483	1.2938	1.2336	1.2326	1.0073	0.7683	0.6427	0.6179	268.0191	329.7961	352.8224	353.6369
	2	1.4036	1.2856	1.2380	1.2366	0.9031	0.7316	0.6356	0.6162	285.8895	335.3699	353.0350	353.6392
	5	1.3570	1.2760	1.2423	1.2407	0.8032	0.6929	0.6276	0.6143	306.1650	341.4871	353.2605	353.6409
	10	1.3248	1.2676	1.2439	1.2425	0.7436	0.6679	0.6223	0.6130	320.1498	345.4847	353.3980	353.6421
8	1	1.1704	1.0608	1.0166	1.0162	0.6447	0.5115	0.4360	0.4206	406.2220	488.8437	520.4413	521.6017
	2	1.1436	1.0572	1.0206	1.0195	0.5899	0.4917	0.4321	0.4196	427.5982	495.4020	520.7057	521.6044
	5	1.1197	1.0533	1.0245	1.0229	0.5445	0.4728	0.4279	0.4185	449.7487	502.5646	520.9969	521.6073
	10	1.0979	1.0475	1.0259	1.0244	0.5120	0.4581	0.4246	0.4177	467.8824	508.1424	521.2008	521.6092
MSGT													
1	1	3.1405	2.7357	2.5808	2.5754	4.7965	3.4504	2.7964	2.6708	57.3878	73.7203	80.1384	80.4195
	2	3.0046	2.7044	2.5883	2.5836	4.1805	3.2390	2.7556	2.6613	62.5984	75.6115	80.1993	80.3560
	5	2.8434	2.6650	2.5952	2.5918	3.5177	2.9943	2.7071	2.6499	69.3934	77.6915	80.2550	80.3605
	10	2.7516	2.6412	2.5979	2.5955	3.1701	2.8573	2.6791	2.6433	73.4413	78.7467	80.3105	80.3885
2	1	1.8701	1.6480	1.5624	1.5600	1.6896	1.2490	1.0274	0.9842	161.3201	203.3851	219.2652	219.8508
	2	1.8008	1.6334	1.5675	1.5651	1.4943	1.1811	1.0142	0.9811	174.1289	207.5845	219.4404	219.8554
	5	1.7223	1.6154	1.5723	1.5701	1.2926	1.1053	0.9989	0.9775	189.7369	212.2785	219.6227	219.8577
	10	1.6737	1.6027	1.5741	1.5724	1.1801	1.0599	0.9895	0.9752	199.6964	215.0353	219.7157	219.8593
8	1	1.2098	1.0929	1.0460	1.0455	0.6911	0.5436	0.4615	0.4448	380.7956	460.7438	491.2166	492.3387
	2	1.1802	1.0885	1.0501	1.0489	0.6299	0.5216	0.4572	0.4437	401.9236	467.2695	491.4820	492.3410
	5	1.1526	1.0837	1.0540	1.0524	0.5773	0.5001	0.4525	0.4425	424.3186	474.4152	491.7706	492.3439
	10	1.1291	1.0774	1.0554	1.0539	0.5410	0.4841	0.4489	0.4417	441.9930	479.7822	491.9658	492.3457

Table 7. Verification studies on the DFFs of the C-C 2D FG porous microbeams for various $p_x, p_z, h/\ell_c$ with constant MLSP ($\alpha_0 = 0.1, \ell_m/h = 0.15, \ell_c = \ell_m$)

L/h	Reference	p_x	FGM I				FGM II			
			$p_z = 0$	1	5	10	$p_z = 0$	1	5	10
12	Present (Q3D TBT, MSGT)	0	26.3981	17.7939	14.5987	13.8740	25.9952	18.0404	14.9844	14.2869
	Present (Q3D TBT, MCST)		24.2721	16.4371	13.5750	12.9163	23.9939	16.7406	13.9797	13.3422
	Karamanli & Aydogdu [53] (Q3D TBT, MCST)		23.7744	15.8815	13.0625	12.4194	-	-	-	-
	Shafiei et al. [47] (FBT, MCST)		23.4313	16.0784	13.4679	12.8762	23.1017	16.2674	13.7621	13.1914
	Present (Q3D TBT, MSGT)	1	17.5715	14.9663	13.6285	13.2829	17.8420	15.3562	14.0621	13.7294
	Present (Q3D TBT, MCST)		16.2566	13.8771	12.6782	12.3630	16.5678	14.2928	13.1253	12.8203
	Shafiei et al. [47] (FBT, MCST)		15.9708	13.7593	12.6710	12.3879	16.1727	14.0523	12.9989	12.7255
	Present (Q3D TBT, MSGT)	5	13.9333	13.3509	13.0199	12.9148	14.3429	13.7927	13.4773	13.3780
	Present (Q3D TBT, MCST)		12.9356	12.4050	12.1139	12.0181	13.3633	12.8620	12.5821	12.4912
	Shafiei et al. [47] (FBT, MCST)		12.8238	12.3764	12.1504	12.0730	13.1442	12.7150	12.4974	12.4234
18	Present (Q3D TBT, MSGT)	0	26.9427	18.1584	14.9290	14.1857	26.5408	18.4246	15.3324	14.6165
	Present (Q3D TBT, MCST)		24.7855	16.7889	13.9100	13.2334	24.5179	17.1138	14.3399	13.6846
	Karamanli & Aydogdu [53] (Q3D TBT, MCST)		24.2657	16.2084	13.3671	12.7092	-	-	-	-
	Shafiei et al. [47] (FBT, MCST)		24.0340	16.4872	13.8296	13.2224	23.7081	16.6915	14.1407	13.5548
	Present (Q3D TBT, MSGT)	1	17.9353	15.2745	13.9244	13.5697	18.2186	15.6803	14.3757	14.0341
	Present (Q3D TBT, MCST)		16.6101	14.1793	12.9755	12.6515	16.9414	14.6180	13.4474	13.1338
	Shafiei et al. [47] (FBT, MCST)		16.3902	14.1134	13.0049	12.7141	16.6070	14.4237	13.3505	13.0697
	Present (Q3D TBT, MSGT)	5	14.2297	13.6312	13.2969	13.1878	14.6564	14.0907	13.7724	13.6694
	Present (Q3D TBT, MCST)		13.2229	12.6796	12.3899	12.2908	13.6741	13.1608	12.8831	12.7889
	Shafiei et al. [47] (FBT, MCST)		13.1531	12.6933	12.4663	12.3870	13.4908	13.0499	12.8315	12.7557

Table 8. Verification studies on the DCBLs of C-C 2D FGM I porous microbeams for various p_x, p_z and α_0 with constant MLSP ($L/h = 40, h/\ell_m = 5, \ell_c = \ell_m$).

α_0	Reference	p_x	p_z				
			0	0.1	0.5	2	6
0	Present (Q3D TBT, MSGT)	0	62.9538	60.0687	53.1933	45.9920	42.0805
	Present (Q3D TBT, MCST)		49.4530	47.2808	42.1386	37.0580	34.3182
	Karamanli & Aydogdu [53] (Q3D TBT, MCST)		46.9072	44.6636	39.2169	33.9166	31.3078
	Shafiei & Kazemi [48] (CBT, MCST)		46.8871	45.1740	40.7701	35.3948	32.6857
	Present (Q3D TBT, MSGT)	2	44.4729	43.6804	41.7338	39.5814	38.3186
	Present (Q3D TBT, MCST)		35.7639	35.1411	33.6382	32.0907	31.1880
	Shafiei & Kazemi [48] (CBT, MCST)		36.1408	35.5349	34.0438	32.2045	31.1964
	Present (Q3D TBT, MSGT)	6	40.2197	39.8632	38.9734	37.9621	37.3525
	Present (Q3D TBT, MCST)		32.5150	32.2330	31.5422	30.8141	30.3789
	Shafiei & Kazemi [48] (CBT, MCST)		33.9678	33.5835	32.6385	31.4597	30.8113
0.1	Present (Q3D TBT, MSGT)	0	58.2258	55.2816	48.2061	40.7907	36.9027
	Present (Q3D TBT, MCST)		45.1704	42.9644	37.6792	32.4571	29.7923
	Karamanli & Aydogdu [53] (Q3D TBT, MCST)		43.4190	41.1079	35.5980	30.2177	27.6552
	Shafiei & Kazemi [48] (CBT, MCST)		43.0365	41.3188	36.8804	31.4834	28.7908
	Present (Q3D TBT, MSGT)	2	39.3063	38.5223	36.5776	34.4122	33.1625
	Present (Q3D TBT, MCST)		31.2656	30.6525	29.1546	27.6030	26.7252
	Shafiei & Kazemi [48] (CBT, MCST)		32.2280	31.6269	30.1477	28.3309	27.3355
	Present (Q3D TBT, MSGT)	6	35.0414	34.6935	33.8142	32.8037	32.2012
	Present (Q3D TBT, MCST)		28.0342	27.7599	27.0782	26.3522	25.9286
	Shafiei & Kazemi [48] (CBT, MCST)		30.0859	29.7043	28.7663	27.59883	26.9563

Table 9. DFFs of the S-S 2D FG porous microbeams for various $p_x, p_z, h/\ell_m$ with constant and variable MLSP ($\alpha_0 = 0.1,\ L/h = 10$)

h/ℓ_m	p_z	MSGT ($\ell = \ell_c = \ell_m$)				MSGT ($\ell_c \neq \ell_m$)			
		$p_x = 0$	1	2	5	$p_x = 0$	1	2	5
FGM I									
1	0	23.0483	16.3983	12.6338	9.2280	34.2388	19.3910	13.4851	9.1927
	1	17.3255	13.0193	10.7896	8.7370	22.7230	14.4710	11.2079	8.6517
	2	14.9792	11.6950	10.0593	8.5362	18.8788	12.7223	10.3396	8.4306
	5	12.1700	10.1617	9.2008	8.2937	14.4409	10.7105	9.3094	8.1587
2	0	13.0233	9.2902	7.1623	5.2339	18.1883	10.6610	7.5532	5.2196
	1	9.6537	7.3145	6.0901	4.9516	12.1686	7.9872	6.2851	4.9149
	2	8.3425	6.5904	5.6958	4.8444	10.1686	7.0676	5.8272	4.7984
	5	6.8926	5.8045	5.2551	4.7188	7.9441	6.0558	5.3056	4.6593
8	0	7.2310	5.2567	4.0799	2.9942	7.9663	5.4416	4.1326	2.9933
	1	5.0861	4.0065	3.4117	2.8237	5.4478	4.1000	3.4398	2.8202
	2	4.3426	3.6299	3.2166	2.7734	4.6080	3.6969	3.2360	2.7686
	5	3.7844	3.3367	3.0471	2.7216	3.9286	3.3703	3.0545	2.7149
FGM II									
1	0	23.9204	17.3502	13.7375	10.4569	35.2794	20.6356	14.8476	10.5717
	1	18.2097	14.0304	11.9164	9.9647	23.7742	15.7012	12.5266	10.0095
	2	15.9592	12.7760	11.2211	9.7719	20.0387	14.0082	11.6776	9.7912
	5	13.2950	11.3343	10.4113	9.5427	15.7493	12.0669	10.6769	9.5263
2	0	13.3925	9.7494	7.7397	5.9108	18.6621	11.2626	8.2522	5.9648
	1	10.0912	7.8446	6.6990	5.6313	12.6950	8.6201	6.9823	5.6533
	2	8.8578	7.1708	6.3289	5.5293	10.7726	7.7423	6.5405	5.5393
	5	7.5007	6.4383	5.9158	5.4109	8.6371	6.7727	6.0369	5.4043
8	0	7.2554	5.3995	4.3395	3.3561	8.0135	5.6059	4.4092	3.3638
	1	5.2508	4.2544	3.7212	3.1935	5.6248	4.3615	3.7606	3.1971
	2	4.5971	3.9263	3.5478	3.1468	4.8722	4.0049	3.5771	3.1487
	5	4.1077	3.6629	3.3924	3.0980	4.2621	3.7066	3.4085	3.0977

Table 10. DCBLs of the S-S 2D FG porous microbeams for various $p_x, p_z, h/\ell_m$ with constant and variable MLSP ($\alpha_0 = 0.1,\ L/h = 10$)

h/ℓ_m	p_z	MSGT ($\ell = \ell_c = \ell_m$)				MSGT ($\ell_c \neq \ell_m$)			
		$p_x = 0$	1	2	5	$p_x = 0$	1	2	5
FGM I									
1	0	110.4851	49.5366	27.7653	14.9418	243.7773	66.0961	30.4720	14.7016
	1	58.3407	30.8197	20.5610	13.5259	100.6907	37.2267	21.7601	13.2005
	2	42.7143	24.8027	17.9738	12.9528	68.1639	28.8957	18.7335	12.5922
	5	27.5413	18.6347	15.1067	12.2625	38.9199	20.5309	15.3592	11.8468
2	0	35.2972	15.9185	8.9331	4.8102	68.8151	20.1793	9.6397	4.7520
	1	18.1011	9.7345	6.5623	4.3486	28.7599	11.3901	6.8819	4.2687
	2	13.2272	7.8775	5.7696	4.1745	19.6552	8.9414	5.9741	4.0850
	5	8.8150	6.0781	4.9285	3.9707	11.7123	6.5714	4.9965	3.8660
8	0	10.9044	5.1228	2.9119	1.5780	13.2281	5.4400	2.9669	1.5748
	1	5.0351	2.9426	2.0759	1.4187	5.7747	3.0686	2.1030	1.4141
	2	3.5920	2.4072	1.8525	1.3714	4.0433	2.4899	1.8706	1.3659
	5	2.6621	2.0163	1.6610	1.3222	2.8685	2.0543	1.6672	1.3153
FGM II									
1	0	125.2037	59.0590	35.2663	20.4849	272.3090	80.3031	39.8900	20.7779
	1	68.0336	38.0756	26.7999	18.7299	116.4113	46.8218	29.1450	18.8236
	2	51.2179	31.4422	23.8356	18.0473	81.1587	37.3325	25.5311	18.0686
	5	34.7279	24.5912	20.5571	17.2373	48.9127	27.6934	21.5002	17.1549
2	0	39.2696	18.6684	11.2086	6.5502	76.2201	24.1102	12.4098	6.6295
	1	20.8765	11.9080	8.4821	5.9866	33.0396	14.1552	9.0960	6.0144
	2	15.7494	9.9048	7.5897	5.7814	23.2989	11.4231	8.0338	5.7897
	5	11.0294	7.9319	6.6381	5.5437	14.6276	8.7300	6.8821	5.5241
8	0	11.5490	5.7543	3.5424	2.1174	14.0816	6.1518	3.6337	2.1240
	1	5.6635	3.5250	2.6352	1.9307	6.4969	3.6911	2.6834	1.9337
	2	4.2505	2.9865	2.3977	1.8765	4.7733	3.1001	2.4328	1.8779
	5	3.3130	2.5749	2.1873	1.8193	3.5666	2.6338	2.2059	1.8185

Table 11. DMDs of the S-S 2D FG porous microbeams for various $p_x, p_z, h/\ell_m$ with constant and variable MLSP ($\alpha_0 = 0.1,\ L/h = 10$)

h/ℓ_m	p_z	MSGT ($\ell = \ell_c = \ell_m$)				MSGT ($\ell_c \neq \ell_m$)			
		$p_x = 0$	1	2	5	$p_x = 0$	1	2	5
FGM I									
1	0	2.2726	4.7644	8.2487	16.3348	1.0301	3.3611	7.1488	16.4427
	1	4.3028	7.8593	11.6699	18.3780	2.4929	6.3046	10.7495	18.7419
	2	5.8781	9.8772	13.5758	19.2923	3.6832	8.2895	12.8002	19.7885
	5	9.1185	13.3154	16.4253	20.4679	6.4523	11.9449	16.0236	21.1655
2	0	7.1180	14.8505	25.6764	50.7901	3.6490	11.1549	22.8613	51.0198
	1	13.8813	24.9545	36.6721	57.2266	8.7329	20.7967	34.2740	58.0908
	2	19.0014	31.1856	42.3879	59.9123	12.7825	26.9931	40.3843	61.0908
	5	28.5211	40.8787	50.3680	63.2416	21.4600	37.4704	49.3666	64.9024
8	0	23.1108	46.4638	79.2490	155.3045	19.0369	43.2545	77.0844	155.3778
	1	50.0523	83.4121	117.1577	176.0372	43.6226	79.5519	115.1651	176.4953
	2	70.1798	103.0785	133.1244	182.8207	62.3261	99.3028	131.4883	183.4797
	5	94.6829	123.8497	149.8063	190.1833	87.8562	121.3625	149.0705	191.1368
FGM II									
1	0	2.0041	4.0387	6.6314	12.0210	0.9213	2.8230	5.6141	11.7525
	1	3.6898	6.4129	9.0651	13.3282	2.1563	5.0822	8.1645	13.2148
	2	4.9021	7.8379	10.3237	13.8825	3.0934	6.4829	9.5047	13.8363
	5	7.2312	10.1216	12.1172	14.5725	5.1338	8.9057	11.5111	14.6343
2	0	6.3974	12.7970	20.8944	37.6344	3.2943	9.4976	18.2262	36.9375
	1	12.0346	20.5533	28.7129	41.7383	7.6014	16.9327	26.3353	41.4288
	2	15.9562	24.9347	32.4788	43.3636	10.7825	21.3108	30.3478	43.2291
	5	22.7899	31.4116	37.5405	45.3353	17.1797	28.3355	36.0269	45.4718
8	0	21.8158	41.7900	66.5860	116.8124	17.8793	38.6842	64.3876	116.2788
	1	44.4854	70.0461	93.2427	129.8086	38.7629	66.5836	91.2474	129.5380
	2	59.2846	83.3451	103.4750	133.8874	52.7762	80.0582	101.7631	133.7459
	5	76.0442	97.1304	114.1628	138.3409	70.6304	94.8285	113.0885	138.3872

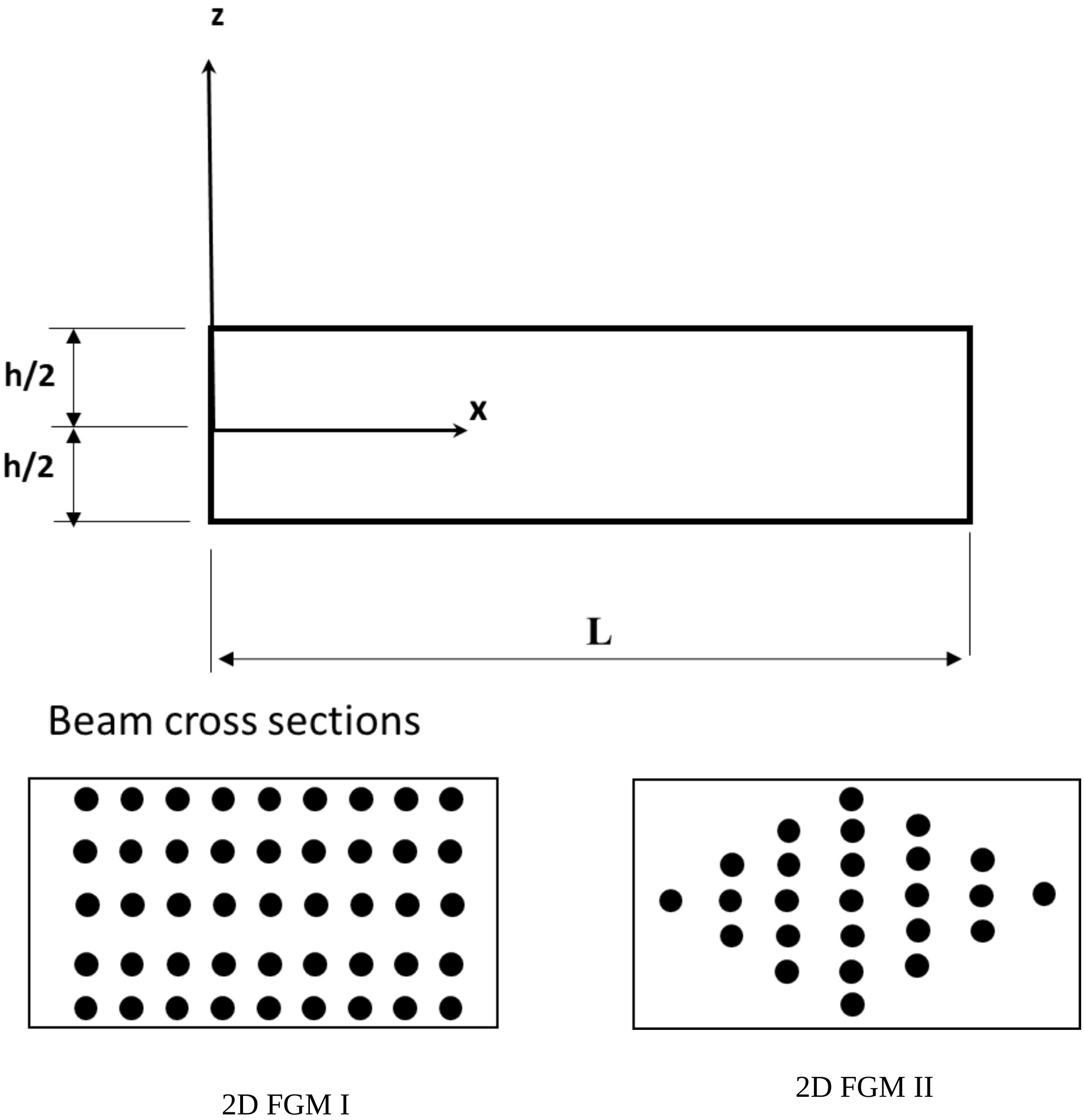

Figure 1. 2D FG porous microbeam models

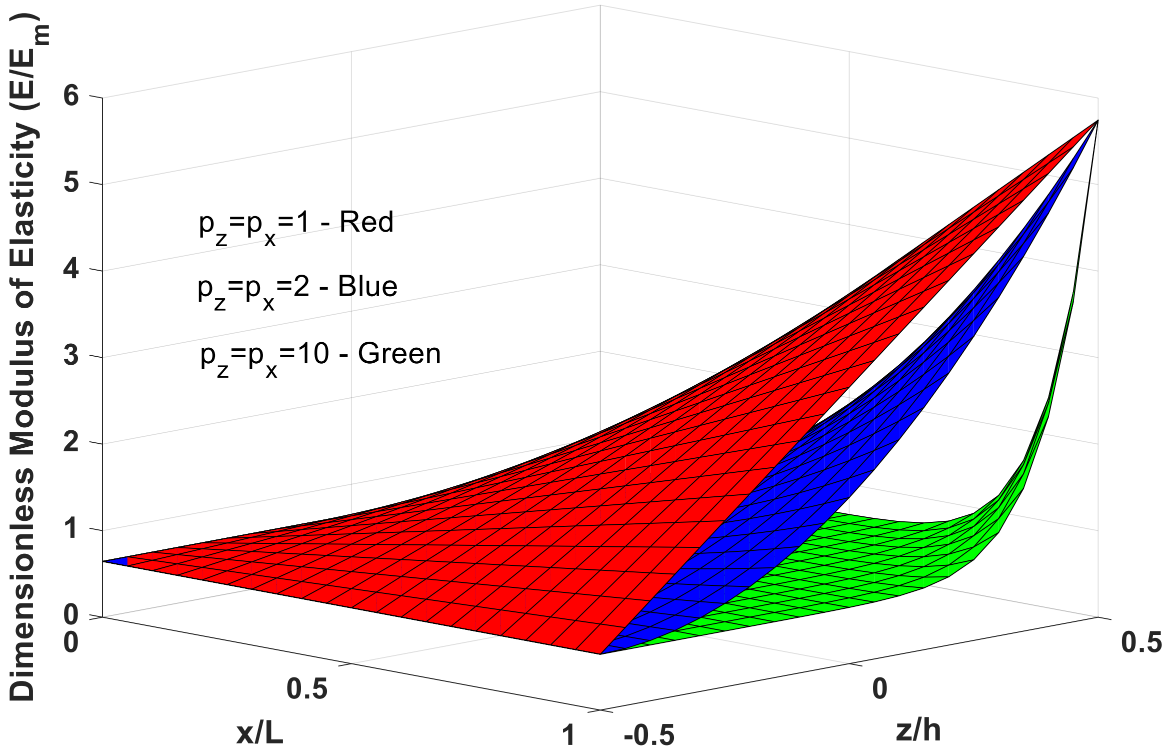

a. Young's modulus of FGM I ($E_m = 70\ GPa;\ E_c = 427\ GPa$)

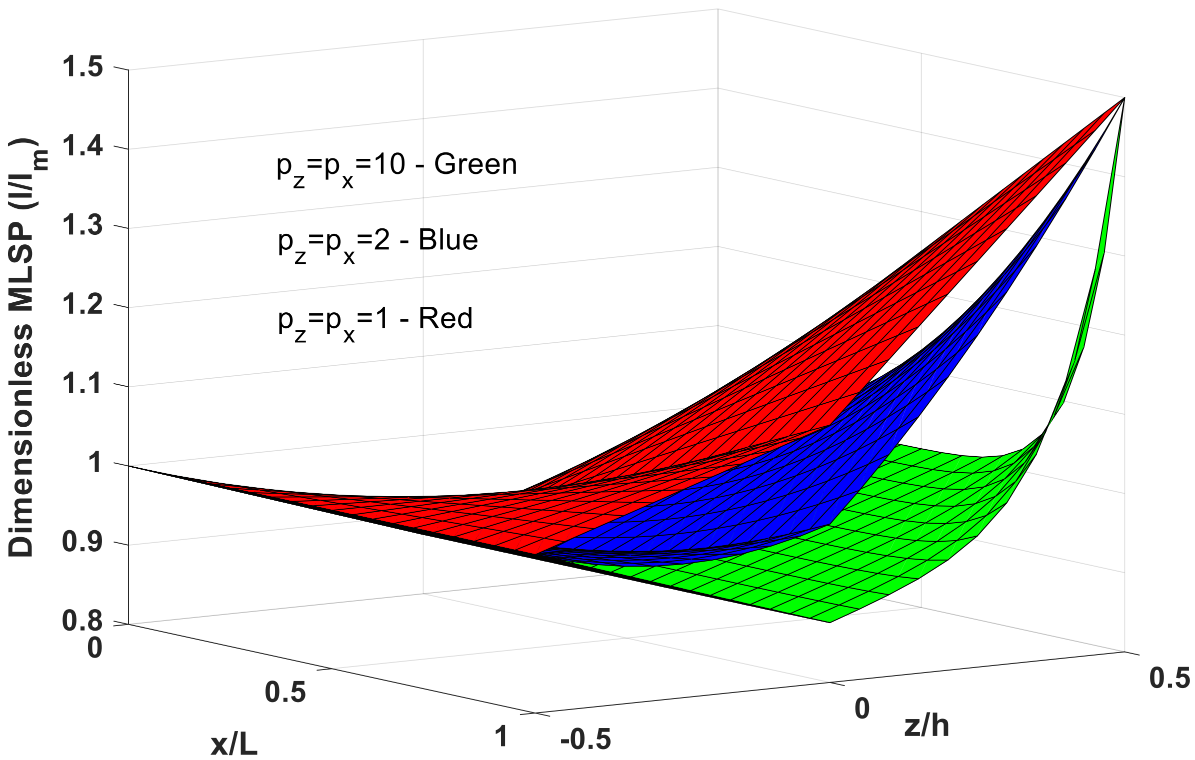

b. MLSP of FGM II ($\ell_m = 15\ \mu m;\ \ell_c = 22.5\ \mu m$)

Figure 2. Variation of Young's modulus and MLSP in *x* and *z*-directions with p_x=p_z=1, 2 and 10 ($\alpha_0 = 0.1$)

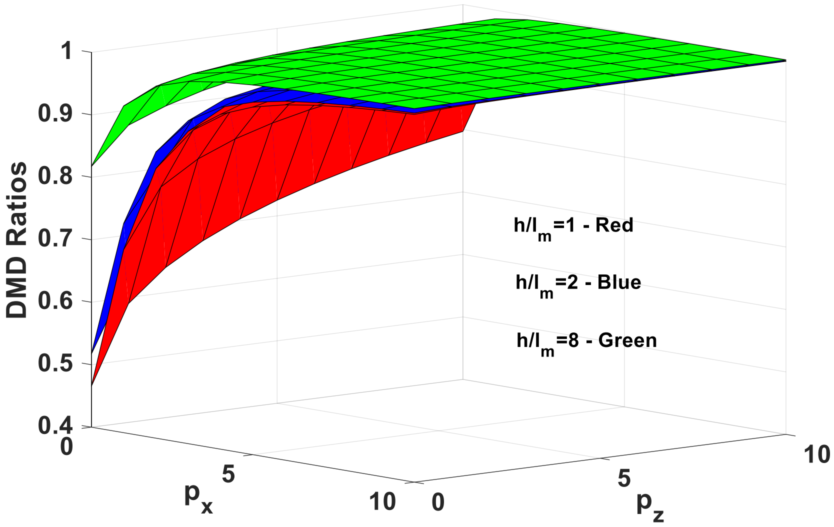

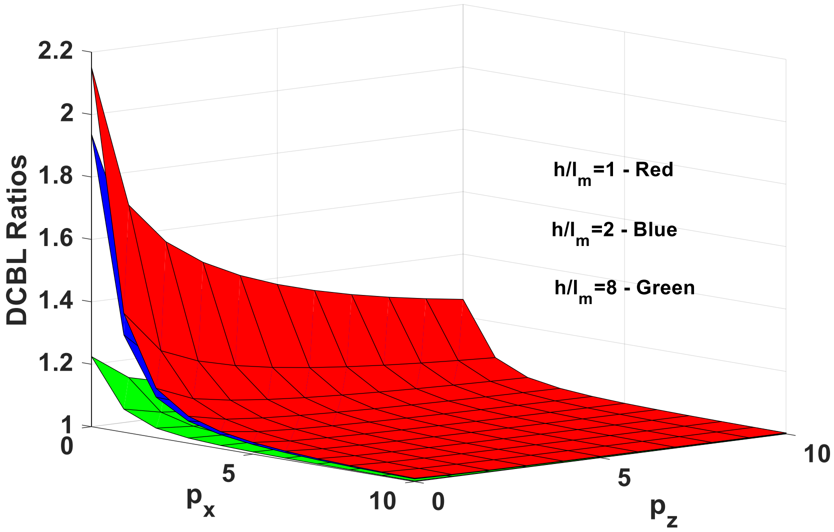

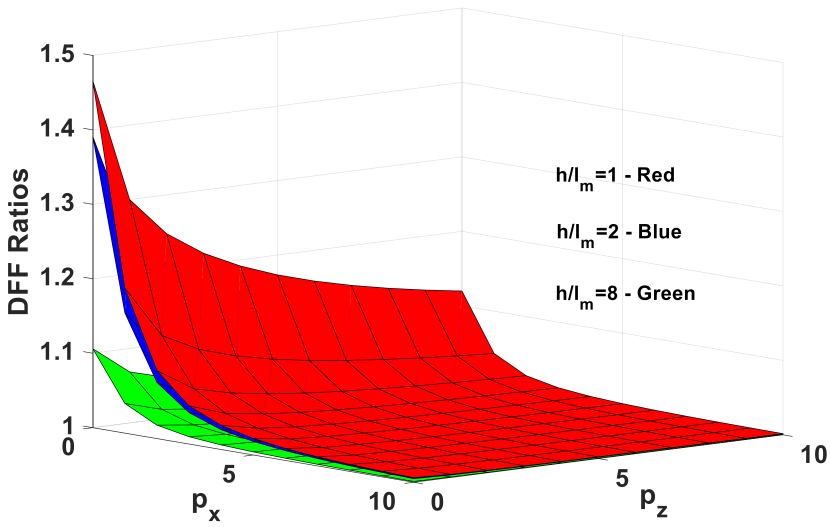

Figure 3. Ratios between the results of S-S 2D FG microbeams obtained from variable and constant MLSP with respect to p_x and p_z $(L/h = 10, h/\ell_m = 1, 2, 8)$

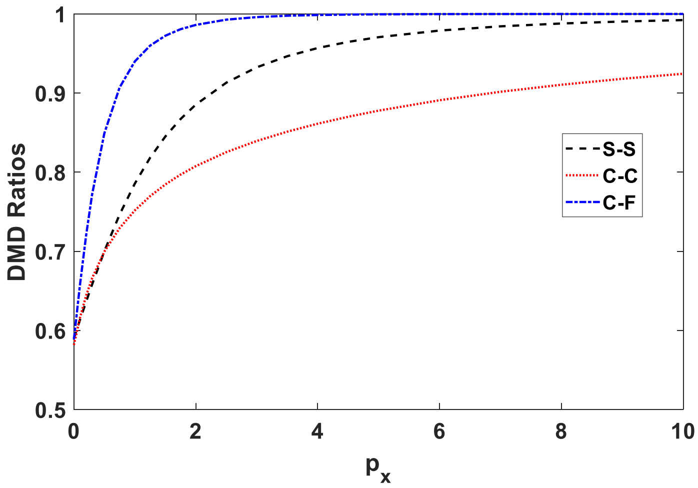

a) $p_z = 1$

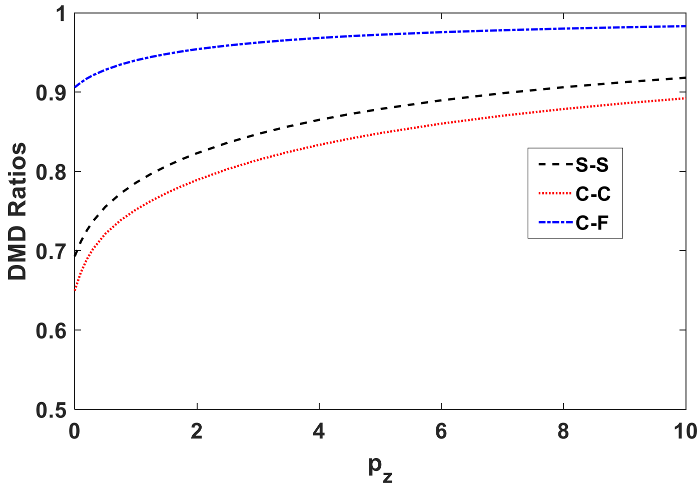

a) $p_x = 1$

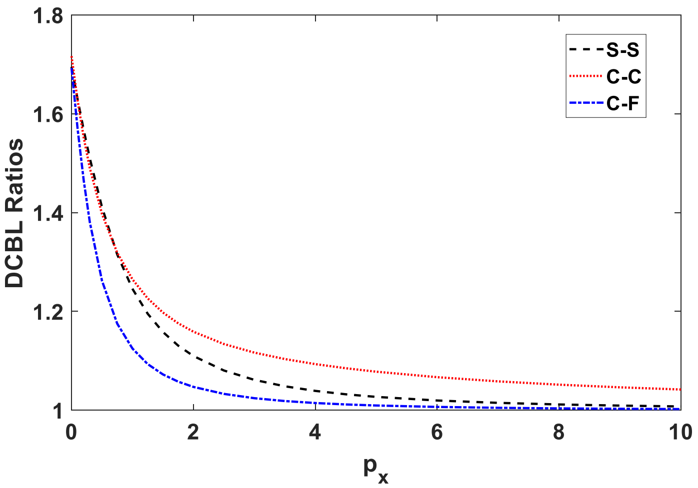

b) $p_z = 1$

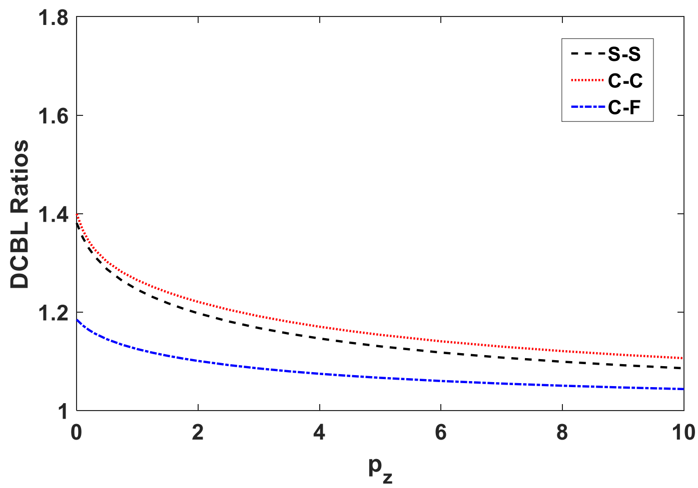

b) $p_x = 1$

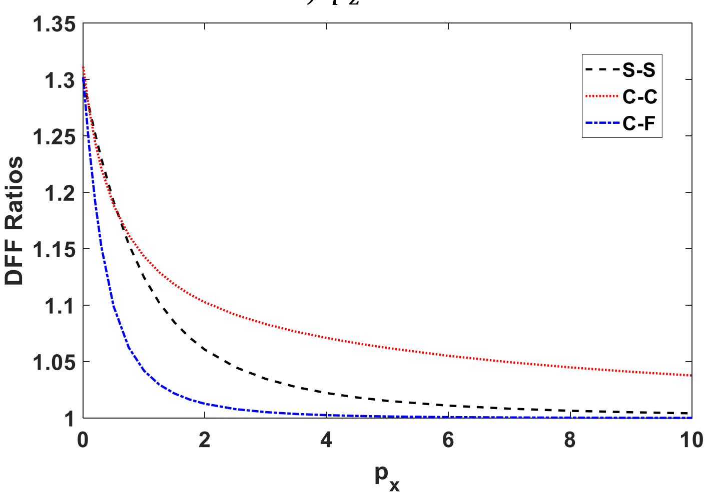

c) $p_z = 1$

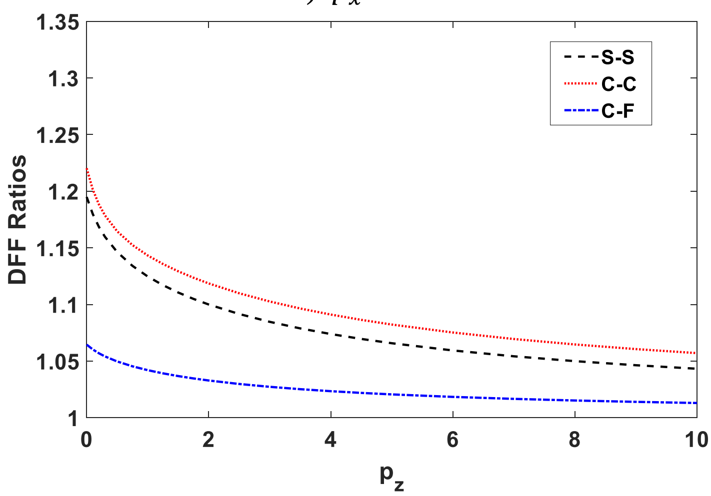

c) $p_x = 1$

Figure 4. Ratios between the results of 2D FG microbeams obtained from variable and constant MLSP with respect to p_x and p_z $(L/h = 10,\ h/\ell_m = 1)$

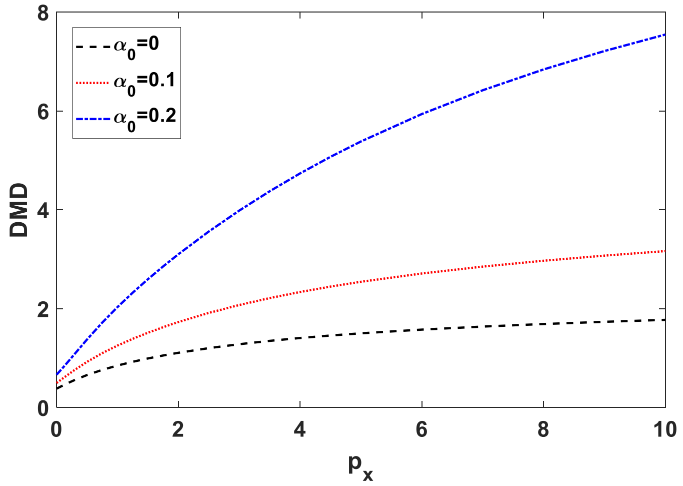

a) $p_z = 1$

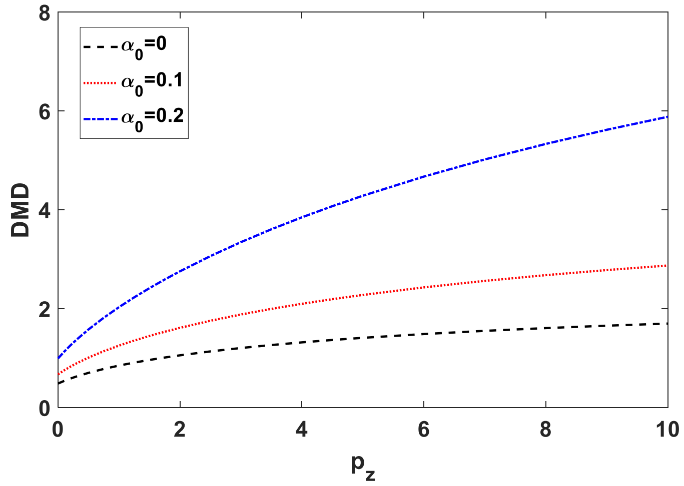

a) $p_x = 1$

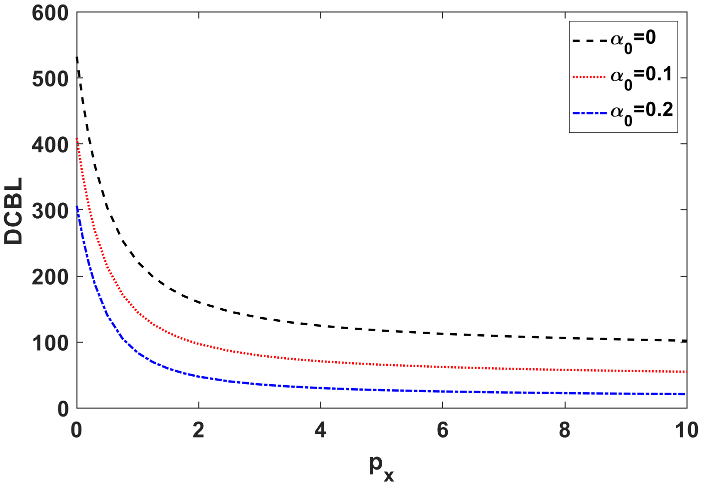

b) $p_z = 1$

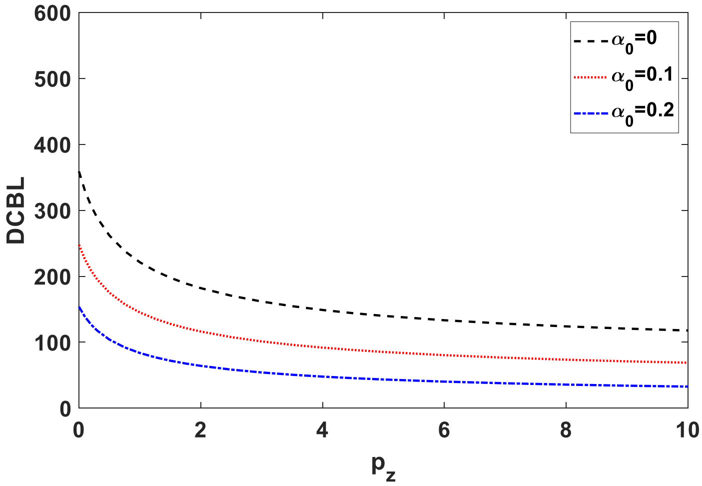

b) $p_x = 1$

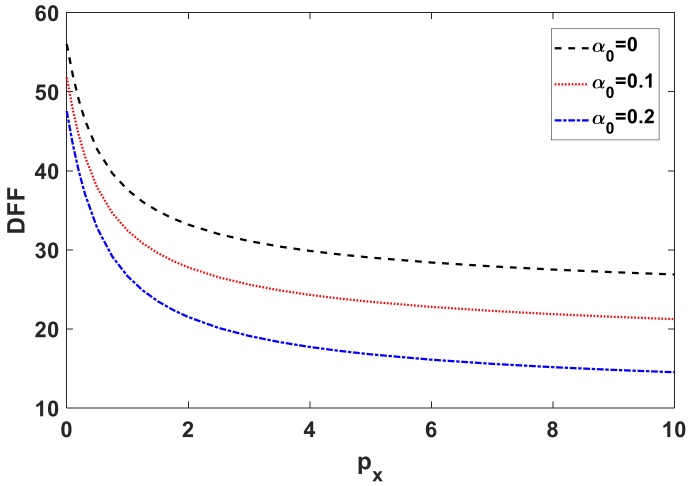

c) $p_z = 1$

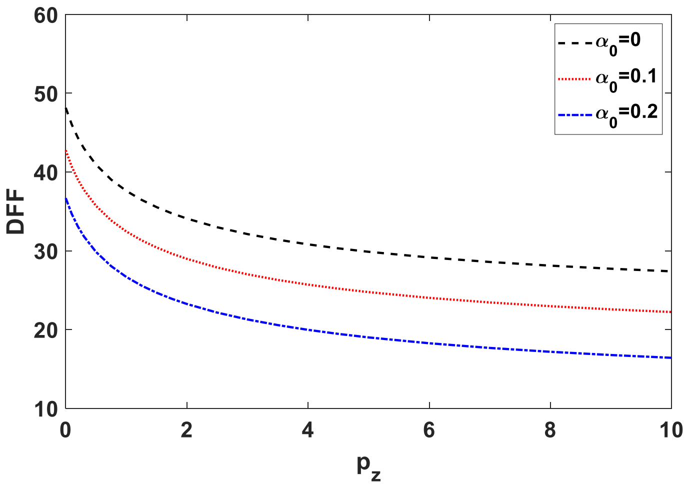

c) $p_x = 1$

Figure 5. DMDs, DFFs, and DCBLs of C-C 2D FGM I porous microbeams with respect to p_x, p_z and α_0 $(L/h = 10,\ h/\ell_m = 1)$

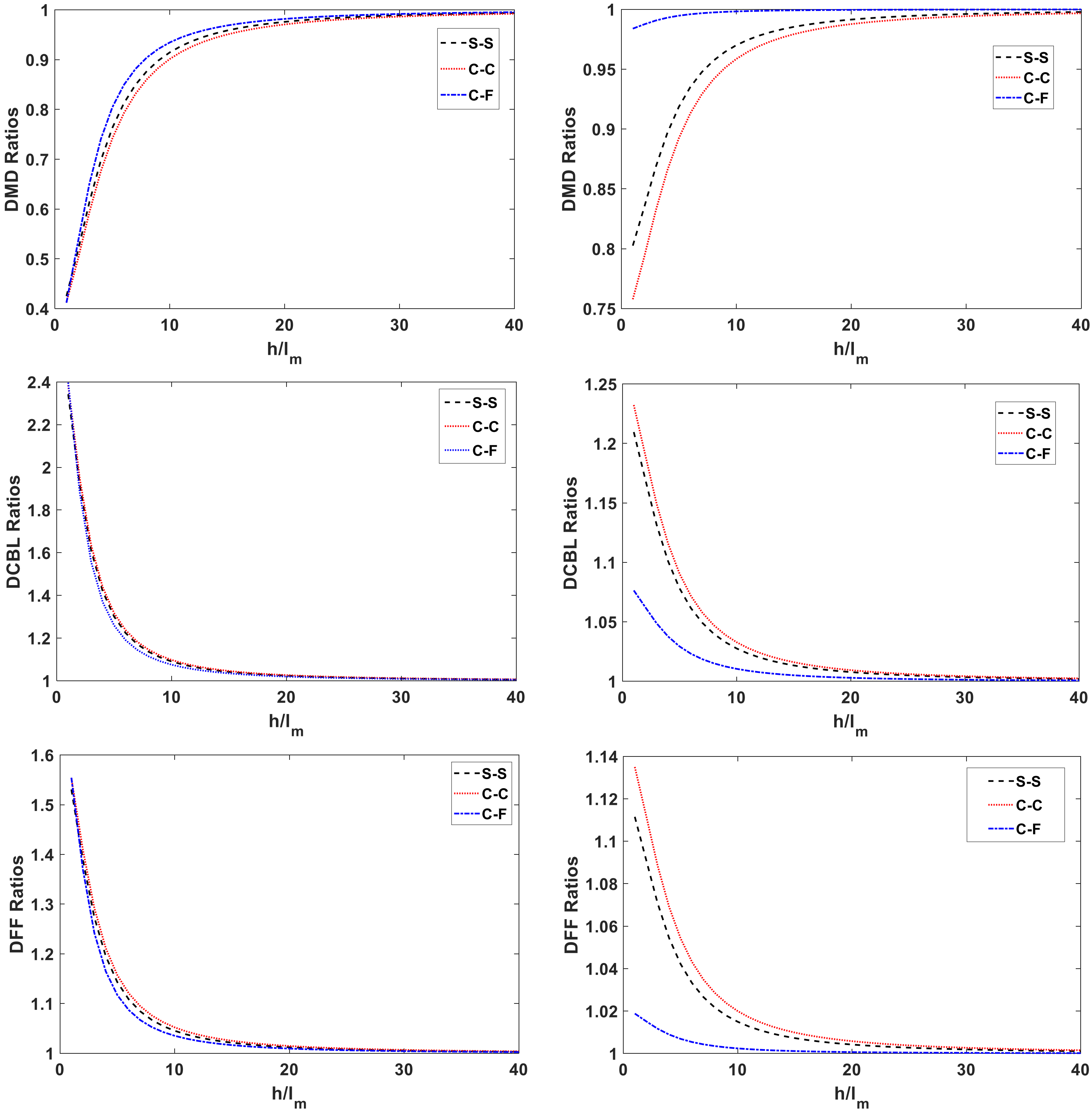

a) Ratios between MSGT and MCST b) Ratios between variable and constant MLSP

Figure 6. Ratios between the results of 2D FGM I porous microbeams obtained from MGST and MCST as well as ratios between those variable and constant MLSP with respect to h/ℓ_m $(L/h = 10, \alpha_0 = 0.1, p_x = p_z = 1)$

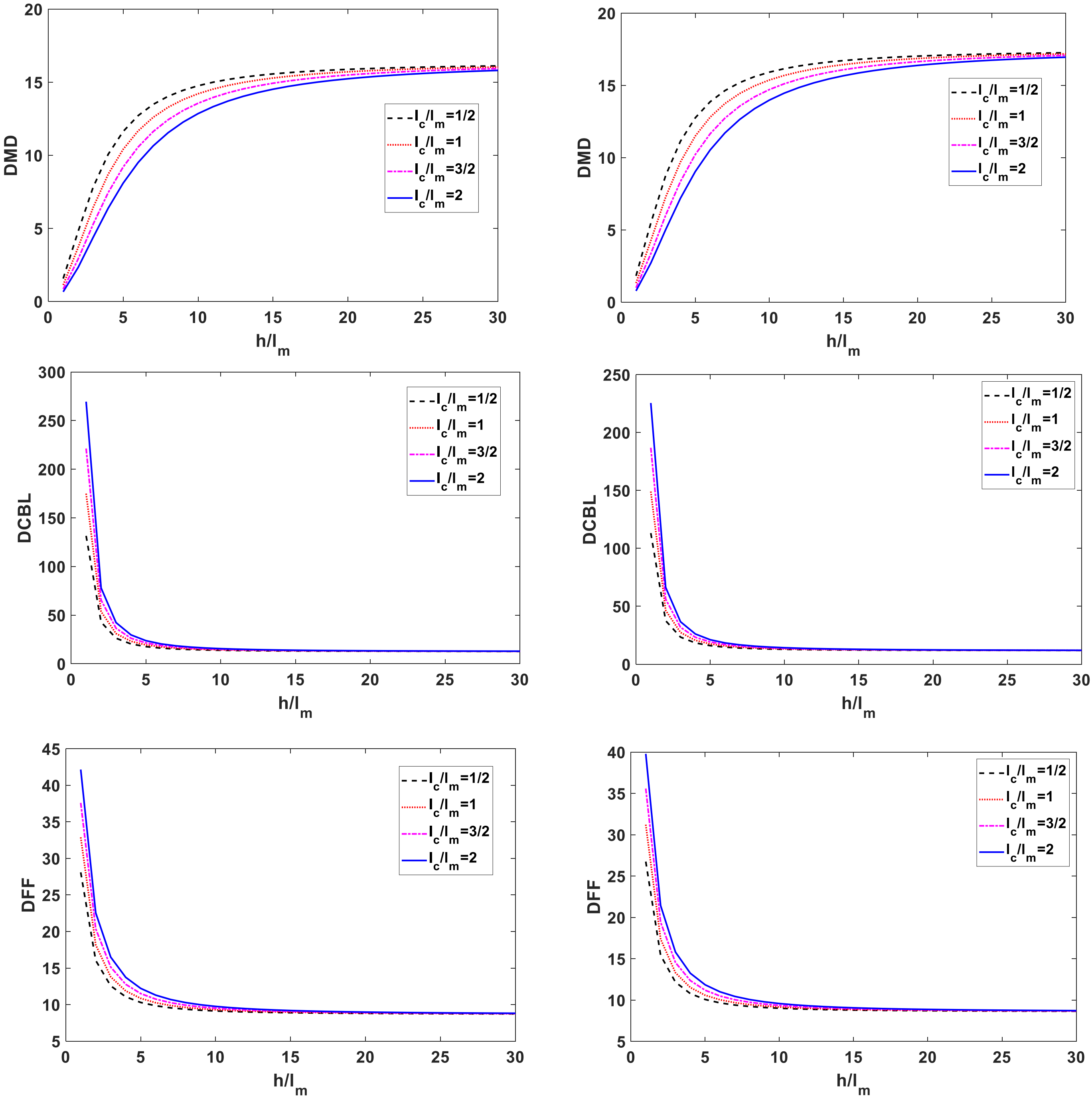

a) FG

b) FGM II

Figure 7. DMDs, DFFs, and DCBLs of C-C 2D FG porous microbeams with respect to h/ℓ_m ($L/h = 10, \alpha_0 = 0.1, p_x = p_z = 1, \ell_c/\ell_m = 1/2, \ell_c/\ell_m = 1, \ell_c/\ell_m = 3/2, \ell_c/\ell_m = 2$)